JPRS-UPM-93-003
4 November 1993

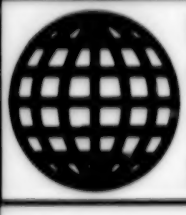

FOREIGN BROADCAST INFORMATION SERVICE

JPRS Report

Science & Technology

Central Eurasia: Physics & Mathematics

Science & Technology
Central Eurasia: Physics & Mathematics

JPRS-UPM-93-003

CONTENTS

4 November 1993

CRYSTALS, LASER GLASSES, SEMICONDUCTORS

GAS DYNAMICS

HIGH-TEMPERATURE PHYSICS

LASERS

MAGNETOHYDRODYNAMICS

NUCLEAR PHYSICS

OPTICS, SPECTROSCOPY

PLASMA PHYSICS

SUPERCONDUCTIVITY

TECHNICAL PHYSICS

THEORETICAL PHYSICS

Epitaxial Characteristics of CdTe/(001)GaAs With Precipitation of Films by 'Hot Wall' Method

937J0101A Moscow IZVESTIYA AKADEMII NAUK RAN: SERIYA FIZICHESKAYA in Russian Vol 57 No 2, Feb 93 pp 120-125

[Article by A. A. Tikhonova, Ye. V. Orlova, U. Syuekhua and D. Ye. Sklovskiy, Crystallography Institute imeni A. V. Shubnikov, Russian Academy of Sciences, Moscow; Fundamental Research Center, Chinese Science and Technology University, Hofei, CPR; UDC 548.52]

[Abstract] The characteristics of epitaxial CdTe films precipitated in a parallel orientation on GaAs (001) substrates are examined (several different orientations are possible, determined by the method for precipitating the film and the conditions for preparing the substrate). Some features of the real structure of films obtained by the "hot wall" method, associated with a nonuniform azimuthal distribution of defects near the heteroboundary, are analyzed. The surface of the substrate and film were investigated by the method of diffraction of high-energy electrons on reflection, whereas the heteroboundaries were studied by high-resolution electron microscopy of transverse film-substrate sections with digital processing of the image. The very same sample was investigated in two perpendicular directions (110). It was found that a network of so-called marginal noncorrespondence dislocations is formed at the interface with a Burgers vector in the interface and there also is a rotation of the film crystal lattice relative to the substrate around one of the directions (110). The rotation is accompanied by the formation of 60° dislocations, complete or dissociated, as well as packing defects. The existence of an azimuthal nonuniformity in the distribution of defects near the heteroboundary is associated with the anisotropy of thermal etching in the process of preliminary annealing of the substrate. Figures 4; references 9: 2 Russian, 7 Western.

Laser-Acoustic Cleaning of Surfaces From Mechanical Microparticles

937J0101B Moscow IZVESTIYA AKADEMII NAUK RAN: SERIYA FIZICHESKAYA in Russian Vol 57 No 2, Feb 93 pp 180-189

[Article by Al. A. Kolomenskiy and A. A. Maznev, General Physics Institute, Russian Academy of Sciences; UDC 534.232]

[Abstract] Since traditional contact methods for the cleaning of surfaces from particles of micron and submicron size are usually a source of additional contamination, laser methods for this purpose are being vigorously developed. The new laser methods eliminate most shortcomings of the contact methods. The detachment of particles measuring tenths of a micron (as small as 0.1 μm) is possible while avoiding contamination, damage or significant surface heating and such processing can now be done in a vacuum. Surface excitation is by an acoustic wave. Another important feature is that the method is not local because the cleaning occurs in the entire region of propagation of the high-amplitude surface wave. As a result, the specific energy expenditures, scaled to a unit area of processed surface, may be far less than in local laser cleaning methods. Another aspect of elimination of particles by laser excitation of powerful short impulses of surface acoustic waves is related to the fact that due to the creation of great accelerations it is possible to overcome adhesive forces of a far greater magnitude than is possible by traditional methods. The appearance of the cleaned region makes it possible to judge the distribution of the acoustic field at the surface. The effect of phonon focusing of surface acoustic waves may play an auxiliary role in the proposed mechanism. As a result, cleaning can be accomplished in narrow strips parallel to the directions of acoustic energy concentration. Figures 6; references 27: 14 Russian, 13 Western.

Characteristics of Radiation of 'MKL-10' Multichannel CO_2 Laser

937J0102A Moscow KVANTOVAYA ELEKTRONIKA in Russian Vol 20 No 3, Mar 93 (manuscript received 25 Aug 92) pp 216-218

[Article by I. V. Babanov, A. F. Glova and Ye. A. Lebedev, Troitsk Innovation and Thermonuclear Research Institute, Moscow Oblast; UDC 621.378.33.038.84]

[Abstract] The lasing power and divergence of radiation of the powerful "MKL-10" multichannel CO_2 laser were measured and optimized. With a near-optimum cavity containing a plane mirror and plane-parallel KCl plate the lasing power was optimized for the output of radiation in gas mixtures (the literature contains no pertinent information on the influence of synchronization of modes on the angular divergence of radiation). The synchronization of laser radiation at the power level 7 kW was achieved by use of a spatial filter. A metal spatial filter with a diameter of the apertures 1.4 mm was positioned in the focus of a telescope formed by a focusing lens with a focal length 191 cm and a concave metal mirror with a radius of curvature 100 cm. The telescope was placed on the side opposite the cavity output mirror. Total efficiency of the synchronization method used can be determined only after allowance for the radiation losses associated with positioning of the optical system and installation of the spatial filter. By use of such a spatial filter a threefold increase in the axial brightness of the radiation was obtained. A further increase in axial brightness can be achieved using wave front phase correctors. Figure 1; references 24: 13 Russian, 11 Western.

Supersonic CO Laser With HF Excitation in Combustion Products

937J0102B Moscow KVANTOVAYA ELEKTRONIKA in Russian Vol 20 No 3, Mar 93 (manuscript received 27 Mar 92) pp 222-226

[Article by G. A. Baranov, I. Ya. Baranov, A. S. Boreysho and I. V. Timoshchuk, Mechanics Institute, St. Petersburg; UDC 621.373.826.038.823]

[Abstract] A preliminary report is given on lasing in a supersonic electric discharge CO laser in combustion products with a power about 12 W with an electrooptical efficiency of about 0.12%. Two experimental designs of such a proposed laser are illustrated and discussed. A table gives the experimental results of lasing experiments in different variants. The first experiment gave low laser output parameters due to the low level of the power contributed to the discharge and the short time of presence of the gas in the discharge zone. An increase in the conveyed power and the extent of the discharge resulted in an appreciable increase in the output power and efficiency of this CO laser. Different buffer gases were used in different experiments. Low lasing efficiencies were attributable in large part to nonoptimum cavity design. Another table gives the output power for different types of CO lasers with similar parameters of the active medium in the cavity, sizes of mirrors and output mirror transmission coefficients. A comparison of the output parameters of the different types of CO lasers indicates that an electric discharge CO laser based on combustion products generates a greater power than chemical and gas-dynamical lasers. The efficiency of a supersonic electric discharge CO laser of this type is equal to the efficiency of an electric discharge CO_2 laser and this affords an approach for the designing of more powerful CO lasers. Figures 4; references 12: 9 Russian, 3 Western.

Source for Photopumping of X-Ray Lasers Based on X-Pinch

937J0102C Moscow KVANTOVAYA ELEKTRONIKA in Russian Vol 20 No 3, Mar 93 (manuscript received 22 Jan 93) pp 237-243

[Article by S. A. Pikuz, B. A. Bryunetkin, G. V. Ivanenkov, A. R. Mingaleyev, V. M. Romanova, I. Yu. Skobelev, A. Ya. Fayenov, S. Ya. Khakhalin and T. A. Shelkovenko, Physics Institute imeni P. N. Lebedev, Russian Academy of Sciences, Moscow; All-Union Scientific Research Institute of Physical Technical and Electronic Measurements, Mendeleyevo, Moscow Oblast]

[Abstract] The use of a high-aperture spectrograph with a spherical mica crystal made it possible to register H- and He-like Al and Si spectra with high spectral and spatial resolutions both in the stage of maximum compression and in the stage of X-pinch plasma expansion. X-ray spectral methods were used in measuring the electron temperature (up to 950 eV) and density (up to 2×10^{24} cm^{-3} at a hot point, as well as the plasma parameters in the stage of plasma expansion. Energy estimates indicated that the emission yield of K lines may be up to 1 J (power 1 GW). The total hot point radiant energy for X-pinch plasma in the wavelength range 0.5-10 nm was about 1 kJ. This is evidence that X-pinch plasma hot point emission may be an efficient source for pumping the X-ray laser working medium and the recombining plasma expanding from the hot region may in itself also be useful as a working medium for short-wavelength lasers. The principal finding of the study is, therefore, that X-pinch plasma can be an effective source of radiation for pumping the active media of X-ray lasers. Figures 12; references 24: 14 Russian, 10 Western.

Highly Efficient Phase Conjugate Mirror Based on InAs in CO_2 Laser Cavity

937J0102D Moscow KVANTOVAYA ELEKTRONIKA in Russian Vol 20 No 3, Mar 93 (manuscript received 15 Sep 92) pp 254-260

[Article by A. E. Vidavskiy, V. I. Kovalev, O. L. Ruskin and M. B. Suvorov, Physics Institute imeni P. N. Lebedev, Russian Academy of Sciences, Moscow; UDC 621.373.826.038.823]

[Abstract] Research with nonlinear media for realization of phase- conjugate reflectance in the 10-micrometer wavelength range by the four-wave interaction method indicated that InAs is the most promising medium for propagation of pulses of microsecond and shorter durations. An experimental apparatus for research along these lines is illustrated and described. The experimentally observed reflection efficiency of the InAs phase conjugate mirror in the cavity of a CO_2 laser was about 200% with a reflection quality about 60% for a signal generated by the radiation of the pumping waves emanating from the cavity. When using the radiation of an independent CO_2 laser as the signal the reflection efficiency was abut 500%, which is the maximum attainable in InAs. The special features of the dynamics of reflection of the phase conjugate mirror during the course of a laser pulse were investigated in detail and particular attention was given to the quality of the phase conjugate mirror. The study confirmed such results obtained in some earlier studies with respect to the lasing parameters of a CO_2 laser with InAs in the cavity as the random character of pulsations of its output power and a short (2-3 ns) duration of the generated peaks, but some other earlier results were refuted. Figures 10; references 15: 14 Russian, 1 Western.

Possibility of Use of Interaction Between Acoustic and Light Waves in Fiber Light Conductors for Generation of Short Light Pulses

937J0102E Moscow KVANTOVAYA ELEKTRONIKA in Russian Vol 20 No 3, Mar 93 (manuscript received 28 Jul 92) pp 276-282

[Article by V. P. Torchigin, Collective Use Computer Center, Russian Academy of Sciences, Moscow; UDC 681.7.068:534.512.1:621.373.826]

[Abstract] Optical cavities based on fiber light conductors with periodic modulation of their refractive indices were investigated. These devices are based on accumulation of the effect associated with a change in phase and therefore also the carrier frequency of a light wave under the influence of a perturbing factor, which results in a

change in the refractive index of the fiber light conductor. Such an influence may be not only the exceedingly weak nonlinearity of the fiber light conductor, but also a change in the refractive index due to LF electric and magnetic fields (although such interactions are very weak). A stronger factor is acoustooptical interaction, in which as a result of change in elastic stresses in the fiber light conductor the refractive index may vary by 0.1-0.01%. A study was therefore made of the possibility of using the mentioned unique features of a fiber light conductor for constructing generators of powerful short light pulses with a wavelength tunable in a wide range on the basis of continuous coherent optical radiation at a fixed wavelength. Such radiation is introduced into a fiber light conductor in which there is modulation of the refractive index by a continuous sinusoidal signal with a frequency less by a factor approximately 10^6 than the frequency of the carrier light wave. Figures 6; references 14: 7 Russian, 7 Western.

Ferron Mechanism of Charge Transfer in Antiferromagnetic Semiconductors and Its Features in Phase Separation

937J0110E Moscow ZHURNAL EKSPERIMENTALNOY I TEORETICHESKOY FIZIKI in Russian Vol 104 No 1(7), Jul 93 (manuscript received 18 Feb 93) pp 2483-2498

[Article by E. L. Nagayev, Institute of High P ressure Physics, Russian Academy of Sciences]

[Abstract] This article presents a theoretical study of the movement of a ferron (the charge carrier in a ferromagnetic region inside an antiferromagnetic semiconductor) in an ideally periodic crystal as it depends on the size of the ferron, the number of electrons in it, and the spin of magnetic atoms. The width of the ferronic band decreases exponentially as its radius increases. In multielectron ferrons, which occur in degenerated antiferromagnetic semiconductors when they divide into ferromagnetic and antiferromagnetic phases, as the number of electrons in the band increases , the band width first increases, then sharply decreases. In imperfect crystals or strong external fields, the movement of ferrons occurs with a hopping mechanism in which the probability of hopping occurring depends on the ferron radius and the number of electrons in qualitatively the same way. The analysis of an experiment using pulsed current in EuTe with phase separation shows that in strong fields ferrons are depinned and form a periodic structure inside the crystal. References 12: 7 Russian, 5 Western.

Acoustic Studies of the Low-Temperature Phase Transition in K_2ZnCl_4 Crystals

937J0111A St. Petersburg FIZIKA TVERDOGO TELA in Russian Vol 35 No 2, Feb 93 (manuscript received 10 Dec 91) pp 265-269

[Article by A. N. Nasyrov, Z. Talchinski, A. D. Karayev, B. A. Agishev, Kh. Shodiyev, Navoi Samarkand State University, Samarkand and the Institute of Physics of Mitskevich University, Poznan, Poland; UDC 537.226.4]

[Abstract] The propagation rates of longitudinal and transverse elastic waves are measured in single crystals of K_2ZnCl_4 at 100-300 K. This temperature interval includes the low-temperature phase transition at 145 K. It is shown that at 145 K the crystal experiences a transition from the Seignette-electric to the Seignette-elastic phase with a corresponding change in the symmetry of the crystal. The phase change is accompanied by the formation of domains in the crystal. The transverse deformation causes the interdomain walls to shift, which results in an increase in the attenuation of a transverse elastic wave as deformation increases. Below the phase transition temperature it is difficult to measure the rate of propagation. A satisfactory agreement between theoretical and experimental results is obtained for a temperature range encompassing the phase transition temperature. Several anomalous results are discussed. Figures 4; references 25: 5 Russian , 20 Western.

Band Inversion in A^4B^6 Semiconductors Associated with Local Stress and Composition Fluctuations

937J0111B St. Petersburg FIZIKA TVERDOGO TELA in Russian Vol 35 No 2, Feb 93 (manuscript received 27 Apr 92) pp 277-284

[Article by B. A. Volkov, A. Ye. Svistov, Lebedev Physics Institute, Russian Academy of Sciences; UDC 537.311.322]

[Abstract] Two mechanisms are examined for the formation of large-scale zonal structure fluctuations which lead to inversion of the terms forming the conductive and valent bands in narrow-gap A^4B^6 semiconductors. The first mechanism is associated with the deformation shifts of bands near point defects, and the other is associated with the presence of large-scale nongaussian fluctuations in the composition of solid solutions which are the basis for A^4B^6 semiconductors. It is shown that in these materials the deformation field of point defects is caused by band inversion in the vicinity of defects. This leads to the formation of an additional resonant level of the point defect, whose energy, in the first approximation, is independent of the type of defect, and which varies with the energy of the main extrema of bands at the *L*-point. It is shown that the presence of large-scale composition fluctuations which accompany band inversions in the solid solutions which are the basis for A^4B^6 semiconductors cause a number of experimental effects which were linked previously with the appearance of deep levels in these compounds. Figures 3; table 1; references 19: 15 Russian, 4 Western.

Nonempirical Cluster Calculations of the Electric Field Gradient Tensor in ^{27}Al Nuclei in $YAlO_3$ and $HoAlO_3$ and Refinement of the Crystal Structure of $HoAlO_3$

937J0111C St. Petersburg FIZIKA TVERDOGO TELA in Russian Vol 35 No 2, Feb 93 (manuscript received 16 May 92) pp 285-289

[Article by L. S. Vorotilova, O. Ye. Kvyatkovskiy, A. A. Levin, B. F. Shchegolev, Grevenshchikov Institute of Silicate Chemistry, Russian Academy of Sciences, St. Petersburg]

[Abstract] The nonempirical cluster method is used to calculate the electron structures and electric field gradient tensor of ^{27}Al nuclei positions for $YAlO_3$ and $HoAlO_3$ compounds. The calculations show a high sensitivity of the electric field gradient tensor to small ch anges in the positions of atoms (when the length of bands changes by 1.5% and the angles between bonds changes by 4.5% in an A lO_6 octahedron, the maximum tensor component changes by 76%, with an average change of about 30%). For known structural data, a good agreement is obtained with NMR data for $YAlO_3$. There is a significant divergence of results for $HoAlO_3$ when X-ray structural analysis of single crystals is used. A satisfactory agreement is obtained between the oretical and experimental values of the electric field gradient tensors with the refined $HoAlO_3$ crystal structure. Tables 2; references 15: 4 Russian, 11 Western.

Spectroscopic Parameters of the Color Centers in $Gd_3Ga_5O_{12}$ Single Crystals

937J0111D St. Petersburg FIZIKA TVERDOGO T ELA in Russian Vol 35 No 2, Feb 93 (manuscript received 18 Jun 92) pp 290-298

[Article by Ya. O. Dovgiy, I. V. Kutyk, A. O. Matkovskiy, D. Yu. Sugak, S. B. Ubizskiy, Franko Lvov State University; UDC 535.37+548.76]

[Abstract] Quantum chemical calculations of the spectroscopic characteristics of vacancy point defects in $Ga_3Ga_5O_{12}$ crystals are used to determine the energies of the corresponding optical transitions, their probabilities, and their broadening. An attempt is made to explain the formation and conversion of color centers in irradiated GdGa garnet crystals based on an approximation of the optical spectra of applied additional absorption using a set of Lorentzian lines with parameters determined from quantum chemical calculations. Figures 3; table 1; references 14: 7 Russian, 7 Western.

Study of the Effect of Laser Annealing on the Structure of Near-Surface Layers of Ion-Implanted Silicon Using X-Ray Diffractometry

937J0111E St. Petersburg FIZIKA TVERDOGO TELA in Russian Vol 3 5 No 2, Feb 93 (manuscript received 28 Jul 92) pp 355-364

[Article by V. A. Bushuyev, A. P. Petrakov, Lomonosov Moscow Stat e University; UDC 548.732]

[Abstract] Diffraction reflection curves and three-crystal X-ray diffractometry are used to stu dy the effect of millisecond laser annealing with varying energy density on the structure of boron-implanted near-surface layers of a silicon single crystal with an energy density greater than 10 J/cm^2. Layer-by-layer scouring is used to determine the effective thicknesses of the affected layer, the middle of the deformation, the type of structural defects, and the amorphization factors. Millisecond irradiation leads to electric activation of the boron in a layer 0.5 μm thick. Defects in this energy density range are predominantly dislocation loops between nodes; at higher energy densities they are dislocation defects. Pulse laser annealing leads to a near-equilibrium distribution of boron atoms in the layer. The presence of structural defects leads to partial or complete amorphization of the near-surface layer. Figures 4; table 1; references 33: 18 Russian, 15 Western.

Effect of Illumination on the Process of 180° Polarization Reversal of $PbTiO_3$ Single Crystals

937J0111F St. Petersburg FIZIKA TVERDOGO TELA in Russian Vol 35 No 2, Feb 93 (manuscript received 30 Jul 92) pp 370-376

[Article by A. F. Semenchev, V. G. Gavrilyachenko, Scientific Research Institute of Physics, Rostov-on-Don; UDC 537.226.33]

[Abstract] It is found that illumination of lead titanate crystals during 180° polarization reversal has both a stimulating and suppressing effect. The former is manifested as a decrease in the coercive field and a decrease in the number of 180° domains involved in the polarization reversal process. The latter is manifested as stabilization of the 180° domain walls and a gradual decrease from cycle to cycle in polarization switching to the complete disappearance of the hysteresis relation *P(E)*. The results are discussed using a well-known model of the polarization reversal of ferroelectric crystals. This model accounts for effects associated with the existence of depleted surface layers, like Schottky layers, and screening of the applied field by free charge carriers. Figures 4; references 15: 10 Russian, 5 Western.

Semiconductor-Metal Transitions in HgMgTe and HgSeS at Very High Pressure

937J0111G St. Petersburg FIZIKA TVERDOGO TELA in Russian Vol 35 No 2, Feb 93 (manuscript received 17 Aug 9 2) pp 389-394

[Article by V. V. Shchennikov, N. P. Gavaleshko, V. M. Frasunyak, Institute of the Physics of Metals, Ukrainian Division, Russian Academy of Sciences, Yekaterinburg; UDC 537.311; 537.32; 536.42]

[Abstract] High-pressure chambers made of synthetic diamonds were used to study the semiconductor-metal phase transitions caused by structural transformations at pressures up to 20 GPa. The replacement of Hg with Mg atoms ($x < 0.1$) has no effect on the pressure of transition into a semiconductor phase. The replacement of Se with S atoms ($0.1 < x < 0.5$) reduces it. The magnetic resistance of the initial semiconductor-metal, semiconductor, and metal phases (> 9+1 GPa) in HgMgTe alloys was measured, which made it possible to qualitatively estimate the change in the mobility of charge carriers in phase transitions. The dependence of resistance and the thermoelectromotive force on pressure was determined. It was found that one can expand the number of materials which experience double metal-to-semiconductor, semiconductor-to-metal transitions under pressure by replacing atoms in the anion and cation sublattices. The substitution makes it possible to increase or reduce the pressure of phase transitions and change the parameters of the electron structure, for example, the width of the forbidden band, not only in the initial phases, but also in the phases formed under pressure. Figures 3; references 20: 11 Russian, 9 Western.

Effect of Thermal Cycling on the Intrinsic Absorption of GaAs

937J0111H St. Petersburg FIZI KA TVERDOGO TELA in Russian Vol 35 No 2, Feb 93 (manuscript received 26 Feb 92; after revision 11 Sep 92) pp 404-407

[Article by G. P. Kovtun, Kharkov Physicotechnical Institute, Ukrainian Academy of Sciences]

[Abstract] This article examines the effect of thermal cycling on the structure of the boundary of intrinsic absorption in electron-conducting GaAs. A shift in the boundary of the fundamental absorption band to lower energies is observed. It is shown that the shift depends on the thermal cycling mode. The absorption spectra of the initial GaAs samples and the thermally cycled samples are presented. The threshold energies of absorption are determined in the initial and thermally cycled samples of GaAs. The results point to an increase in the density of defects caused by the creation of large internal tension fields during thermal cycling. Thermal cycling makes it possible to change the electrophysical characteristics of GaAs samples, and consequently, the electrophysical properties of semiconductor compounds in general, by changing their defect structures. Figure 1; table 1; references 10 (Russian).

Steady Three-Dimensional Flow of Viscous Gas Through Channels and Nozzles

937J0107D Moscow TEPLOFIZIKA VYSOKIKH TEMPERATUR in Russian Vol 31 No 3, Jun 93 (manuscript received 22 Oct 92) pp 395-405

[Article by A.Ye. Kuznetsov, M.Kh. Strelets, and M.L. Shur, Institute of Applied Chemistry, St.Peterburg; UDC 519.6:533.7]

[Abstract] The steady-state solution to the system of Navier-Stokes three equations describing three-dimensional flow of a viscous compressible gas in generalized curvilinear coordinates is obtained by the method of finite differences using an implicit scheme, following separation of the space coordinates and division of the physical process along each. In the case of arbitrary generalized coordinates there appear additional terms in these equations. Implicit approximation of these terms, necessary for ensuring an adequately high stability of the scheme, requires three-point elimination of not only scalar but also vector variables for simultaneous solution of the continuity equation and the impulse balance equation. The resulting scheme for numerical analysis is of second-order precision along the space coordinates and remains universal with respect to the Mach number. For illustration, this scheme is applied first to isometric flow of an incompressible fluid through a channel with a 90° bend and then to flow of a compressible gas through a deLaval nozzle at velocities up to Mach 4. Figures 13; references 20.

Experimental Study of Thermal Breakdown of Silicon Nitride

937J0107F Moscow TEPLOFIZIKA VYSOKIKH TEMPERATUR in Russian Vol 31 No 3, Jun 93 (manuscript received 25 Jan 93) pp 444-449

[Article by V.A. Tovstonog, Moscow State Technical University imeni N.E. Bauman; UDC 536.421]

[Abstract] An experimental study of silicon nitride was made concerning its breakdown with attendant decomposition $Si_3N_4 \rightarrow 3Si + 2N_2$ when heated by intense radiation to and above T_D= 2170 K, up to which temperature it remains thermodynamically stable. As the heat source was used a laser module delivering a total power of 350 W through a shutter. An array of lenses focused the beam of heating radiation on the test specimen with a usual nonuniform radial power density distribution. Specimens of loosely packed and randomly oriented Si nitride fibers (density of solid fiber about 3200 kg/m^3) with an apparent density of approximately 300 kg/m^3 were tested. Random orientation of the fibers made the specimen material virtually isotropic and owing to the very small fiber radius, about one thousandth of the laser beam radius, the material was responding to incident radiation as a virtually homogeneous one. The very low thermal conductivity of this material ensured minimum heat dissipation. Interaction of the material and the incident heating radiation was monitored by a multichannel recording instrument with synchronization of channels. One channel was assigned to signals from the shutter, for monitoring the incident radiation. Three other channels were assigned respectively to signals from two photoconductive cells and one photomultiplier with an input filter each, for monitoring the radiation emitted by the hot spot of the specimen and by the flame of decomposition products. The photomultiplier and one photoconductive cell were oriented at an about 10° angle to the laser beam axis while one photoconductive cell was oriented transversely to it. One channel was assigned to signals from a probing optical system measuring the transmission characteristics of the flame of decomposition products. This probing optical system consisted of an LG 66 gas laser with a beam modulator followed by two plane mirrors, each oriented at 45° to the beam axis. The semitransparent beam-splitting first mirror deflected one part of the probing laser beam to a photomultiplier (without filter), which sent its output signals through a narrow-band amplifier to a single-channel recording instrument, and transmitted the other part of that beam without deflection to an opaque second mirror. This opaque mirror reflected that part of the probing beam through the telescope of an optical pyrometer onto the camera, an RFK-5 time-lapse camera operating at a 5-10 Hz pulse frequency. The changing brightness temperature of the flame was read on successive photographs and the readings were sent into the so assigned channel of the main recording instrument. The mass rate of wear as principal quantitative parameter of the Si nitride breakdown was determined from the loss of mass after successive exposures to pulses of incident heating radiation and from the geometrical dimensions of the crater. The evaluation of experimental data is combined with a theoretical analysis, considering that the chemical decomposition reaction most likely proceeds in several stages. Inasmuch as reliable information of the attendant processes is lacking, this analysis is based on the model of Si_3N_4 dissociation into nitrogen and residual silicon condensate (melting point 1688 K < T_D, boiling point 3522 K > T_D). Heating to the dissociation temperature T_D is treated as a two-dimensional process and is described by the partial differential equation of heat conduction in cylindrical coordinates [x,r] with the initial condition T= T_0 at time t= 0. This equation is solved for a body occupying an entire half-space and a laterally bounded normally incident radiation beam with a known radial distribution of the radiant flux density. The solution to this equation yields the time to reach the dissociation temperature T_D. The effective reaction activation energy is estimated on the basis of the equation $d\alpha/dt = kf(\alpha)$ describing the kinetics of condensate decomposition ($k = k(0)e^{-E/RT}$- reaction rate constant, R- gas constant, E- activation energy, T- temperature). For solving this equation it is necessary to determine the not a`priori known mode of temperature rise during the heating period, which cannot be done on the basis of already available experimental data but requires special indirect measurements. The surface temperature of the specimen is estimated by regarding the breakdown process as a quasi-steady one and calculating its parameters on the basis of the locally one-dimensional double-layer model, considering also that in such a process the rate of silicon evaporation is equal to the rate of silicon production by dissociation of its nitride. The partial pressure of silicon vapor is calculated in the "frozen xSi + yN composition" approximation and also in the "equilibrium 3Si + 4N composition" approximation, the equilibrium composition being possibly limited by presence of Si_2 and Si_3 molecules along Si and N_2 at temperature of 2000-4000 K. Figures 5; references 11.

Evaluating Characteristics of Thermal Interaction of Materials With Two-Phase Stream by Inverse Problem Method

937J0107G Moscow TEPLOFIZIKA VYSOKIKH TEMPERATUR in Russian Vol 31 No 3, Jun 93 (manuscript received 21 Oct 92) pp 450-454

[Article by O.M. Alifanov, Ye.A. Artyukhin, A.V. Nenarokomov, and I.V. Repin, Moscow Institute of Aviation; UDC 533.6.011.6]

[Abstract] Interaction of materials and two-phase stream (fluid carrying solid particles) with attendant mass and heat transfer is analyzed on the basis of experimental data and a mathematical model. For illustration is considered a hollow cylindrical probe open at one end and closed by a flat wall at the other end, this wall interacting with an axially flowing high-enthalpy stream of a fluid carrying solid particles. The heat transfer inside the probe is described by the one-dimensional

equation of heat conduction, boundary conditions of the first kind being satisfied at the inside wall surface and the boundary condition of heat balance $q_k = -k(\delta T/\delta x)_w = q_{conv} + q_{turb} + q_{rough} + q_{kk}$ being satisfied at the outside wall surface (q_k- density of thermal flux heating the probe within the stagnation region, k- thermal conductivity of the probe material, ω_{conv}- density of convective external thermal flux, q_{turb}- density of thermal flux generated by additional turbulence due to presence of solid particles, q_{rough}- density of thermal flux increment due to increase of surface roughness, q_{kk}- density of thermal flux increment due to accommodation of the kinetic energy of solid particles). The unknown values of parameters in the either theoretical or empirical relations for these four components of total thermal flux density are determined upon solution of the inverse heat transfer problem by the method of iterative regularization, the vector of those unknown values being required to satisfy the mathematical model $c(T_n/\tau) = (\delta k/\delta x)\delta T_n/\delta x)$ (x- axial space coordinate, τ- time, c- specific heat, k- thermal conductivity) after their measurement in a successive experiments with M_n thermocouples in each n-th experiment. The tem, .rature dependence of both specific heat c(T) and thermal conductivity k(T) are assumed to be known. The procedure, including a numerical analysis, is demonstrated on cylindrical probes made of M2 copper with an 80 cm outside diameter and various initial wall thicknesses. Figures 1; tables 2; references 7.

Vortex Cooling of Heated Channel in Compressible Gas

937J0107E Moscow TEPLOFIZIKA VYSOKIKH TEMPERATUR in Russian Vol 31 No 3, Jun 93 (manuscript received 16 Jul 92) pp 406-410

[Article by M.N. Shneyder, All-Russian Scientific Research Center at All-Russian Institute of Electrical Engineering; UDC 537.523:539.9:532]

[Abstract] Isobaric cooling of a heated channel in a compressible gas is considered, a model of this process being proposed which includes both generation and dissipation of turbulence. Accordingly, a cylindrical hot channel is immersed in an initially quiescent "cold" gas, whereupon the supply of heat needed for maintaining the channel in a quasi-steady state is discontinued at some time t= 0. As the temperature of the channel falls, the density of the gas increases and cold gas needs to be drawn from the periphery of the channel toward its axis. The flow is unstable, inasmuch as macroscopic motion of a gas under such conditions is inevitably vortical. Preliminary estimates indicate that turbulence is generated with negligible delay and the kinetic energy of the incoming gas is immediately converted into kinetic energy of turbulent fluctuations, some energy being lost on viscous damping. All parameters characterizing the macroscopic properties of the gas inside the channel are assumed to have constant mean values in each cross-section. The largest Reynolds number in the turbulence channel is $N_{Re}= u_{max}r/\nu(T) = 100$ (u_{max} being the r.m.s. velocity of largest-scale turbulent fluctuations, ν being the temperature-dependent kinematic viscosity of the gas, r being the radial coordinate in the channel). This empirical relation fits the conditions of known experiments. Inasmuch as the energy of a unit gas volume is the sum of kinetic energy and internal energy, the rate of change (time derivative) of each is described by a separate partial differential equation. The right-hand side of each equation consists of a divergence with a minus sign and a term representing dissipation of kinetic energy into heat caused by viscous damping. This term has also a minus sign in the equation of internal energy and a plus sign in the equation of kinetic energy. The divergence term in the equation of kinetic energy includes energy transfer by molecular heat conduction and loss of energy by radiation. Assuming that throughout the entire cooling process practically all the entire energy of turbulent fluctuations concentrated in large vortices without spectral diffusion, the cooling problem is in this approximation solved by integration of those two equations. Cooling of a laser-spark channel in air has analyzed numerically on the basis of this model. The authors thank Yu.P. Rayzer and A.A. Perunov for helpful discussions. Figures 5; references 9.

Pulsed Chemical HF-Laser With γ-Radiation Pumping

937J0108A Moscow DOKLADY AKADEMII NAUK in Russian Vol 331 No 3, Jul 93 (manuscript received 2 Mar 93) pp 299-301

[Article by Academician A.I. Pavlovskiy (deceased), Ye.K. Bonyushkin, V.V. Varaksin, V.S. Vinyarskiy, A.Ye. Lakhtikov, G.M. Mishchenko, A.P. Morovov, and V.D. Urlin, All-Russian Scientific Research Institute of Experimental Physics; UDC 621.373.826.038.823]

[Abstract] An experimental study of a SF6 + H2 laser longitudinally pumped by hard γ-radiation produced by nuclear explosion was made, the gaseous active mixture occupying a cylindrical 480 cm long and 11 cm in diameter cell without resonator under a total pressure of 2.1 atm, (9:1 ratio of partial sulfur hexafluoride and hydrogen pressures). The radiation beam was oriented at a 10° angle to the cell axis and its divergence ws minimized by having the 60 cm front segment of the cell split into a tight bundle of longitudinal shaper channels 0.3 cm in diameter each. The γ-radiation beam was oriented at a 10° angle to the cell axis. The laser was tested in the single-pass amplifier mode with a traveling initiation and emission wave, an about 1 J/cm^3 mean-volume input energy provided by γ-radiation pump pulses of 18 ns total duration. The emission energy was measured with grid bolometers using 10 μm thick filaments as sensors. The time-average angular divergence of the laser beam was determined from the radial distribution of its energy in the far zone, the energy there being measured with an array of calorimeters. The form of the laser emission pulses was determined with the aid of a pyroelectric detector using a ferroelectric sensor. On the basis of these measurements were obtained a 4.4 J/cm^2 energy density at the exit from the active medium, a 7 mrad angular laser beam divergence, and an 8 ns laser pulse width at half-amplitude. The subsequent analysis of the experimental data was based on the theoretical model of a pulsed HF-laser, the speed of rotational relaxation being finite. They were thus analyzed first in the usual one-dimensional approximation of the radiation transfer equations for forward wave and backward waves on working P-transitions in a n HF molecule, the results indicating that de-excitation takes place in the direction of propagation of the traveling trigger wave. They were then analyzed, accordingly, by treatment of a thus triggered laser as a thin cylinder with nonreflecting walls. Evolution of laser emission in the shaper channels was simulated in the spherical-wave approximation, a gain of at least 0.25 cm^{-1} having been found to be required for the intensity of laser emission to appreciably exceed that of spontaneous radiation emission. This condition is realizable only on seven working transitions in an HF molecule: $P_1(4)$, $P_1(5)$, $P_3(3)$, $P_2(4)$, $P_2(5)$, $P_2(6)$, $P_2(7)$. The radiation signal emitted by this laser is, therefore, the sum of two signals: one whose divergence is determined by the geometry of the shaper channels and one with a broader radiation pattern. The authors thank R.A. Orlov, V.T. Sinyapkin, and V.P. Yaichkov for assistance in the measurements. Figures 2; references 3.

Nonlinear Dynamics of a Ruby NMR Laser With External Feedback

937J0110D Moscow ZHURNAL EKSPERIMENTALNOY I TEORETICHESKOY FIZIKI in Russian Vol 104 No 1(7), Jul 93 (manuscript received 15 Oct 92) pp 2314-2329

[Article by N. A. Loyko, A. M. Samson, Stepanov Institute of Physics, Belarusan Academy of Sciences]

[Abstract] This article presents a theoretical model of a ruby NMR laser with an injected signal controlled by a delaying feedback. Based on the difference-differential equations which are developed, the lasing dynamics are studied in detail. The conditions for the generation of stable pulses and their characteristics are determined. It is shown that at relatively large feedback depths a cooperative configuration of fields is achieved (the phase difference between the field which is generated and the injection field is zero). As in the case of a signal which is constant over time, this configuration is characterized by stable solutions. The results which are obtained indicate that the laser system examined here substantially enriches the spectrum of lasing modes in a ruby NMR laser. This expands the laser's area of application and the possibility of using it to study bifurcation phenomena, multistability and the generation of chaos. Figures 5; references 14: 5 Russian, 9 Western.

Numerical Study of Properties of Combustion Products of Pulverized Fuels for Pulsed MHD Generators

937J0104A Moscow TEPLOFIZIKA VYSOKIKH TEMPERATUR in Russian Vol 31 No 2, Apr 93 (manuscript received 17 Sep 92) pp 229-234

[Article by Yu. G. Degtev and V. P. Panchenko, Troitsk Institute of Innovative and Thermonuclear Research, Troitsk, Moscow Oblast; UDC 662.61.25:533.932+621.362]

[Abstract] The results of numerical research on the electrophysical properties of the combustion products of pulverized carbon, aluminum, boron, magnesium and their mixtures with addition of salts of alkali metals (K_2CO_3 and KNO_3) in oxygen and air are presented. An intercomparison is made and a comparison also is made with similar parameters of combustion products of solid plasma- forming fuels and liquid metallized fuels based on kerosene with their combustion in oxygen and air. It is shown that a fuel based on pulverized metals (aluminum, magnesium and their mixtures) with combustion in the air, as well as pulverized carbon with its combustion in oxygen, is of the greatest interest for pulsed MHD generators. The highest computed conductivity σ and energy complex σv^2 values (v is the flow velocity) of the combustion products are attained with the combustion of aluminum in air. With a pressure in the combustion chamber P_k about 4 MPa in the range of Mach numbers about 3 these values are σ about 85-130 mho/m, σv^2 about 450-690 (mho/m)(km/s)^2 and electron mobility μ_e about 0.7-0.9 Tl^{-1}. The electrophysical properties of the combustion products of a fuel based on magnesium differ from those of a fuel based on aluminum by less than 30%, but have a temperature less by 400-500 K in the combustion chamber. Figures 3; references 12: 10 Russian, 2 Western.

Current Transfer in Ceramic of Combined Electrodes and Interelectrode Gap of MHD Generator

937J0104B Moscow TEPLOFIZIKA VYSOKIKH TEMPERATUR in Russian Vol 31 No 2, Apr 93 (manuscript received 12 Jul 90) pp 321-327

[Article by L. N. Rudenko and L. S. Simonenko, Power Conservation Problems Institute, Kiev; UDC 621.313.522]

[Abstract] This article, representing a continuation of an earlier study by the authors (TVT, Vol 27 No 6, p 1238, 1989), gives the results of research on distribution of the current flowing on the edges of the metal framework and ceramic filler of a combined electrode and also in the volume of the interelectrode insulator and ceramic filler of the electrode with a change in magnetic field induction B from 0 to 1.8 Tl. The results obtained in a field created by an external emf with B = 0 are given as a comparison. Data were obtained on the dynamics of change in the resistivity of a plasma-sprayed Al_2O_3 layer on the lateral metal surface of the electrode, interelectrode gap of MgO ceramic and ceramic filler of electrodes from materials based on ZrO_2 or $LaCrO_3$ in the course of operation of a MHD channel. The methodology of the experiments and the equipment used are described and the technical specifications of the electrodes are given. The principal current load on a combined electrode without a special current output falls on the upper sectors of the metal edges and the ceramic zones adjacent to them (2-4 mm over the surface and in depth). The direction of the electric and magnetic fields substantially changes the current distribution over the surface of the electrode but exerts virtually no influence on the flowing of current at a depth greater than 3-4 mm from the surface. Potassium compounds penetrating into the ceramic in the course of operation of a MHD channel increase its conductivity by two or three orders of magnitude. The proposed method for measuring the current distribution over the surface and in the volume of the electrode wall make it possible to obtain data on the condition of the electrode wall in the course of operation of a MHD generator channel. Figures 8; references 16: 12 Russian, 4 Western.

Counterflow in Water-Moderated Water-Cooled Nuclear Reactor Core

937J0104C Moscow TEPLOFIZIKA VYSOKIKH TEMPERATUR in Russian Vol 31 No 2, Apr 93 (manuscript received 14 May 92) pp 330-333

[Article by B. L. Kantsyrev and B. I. Nigmatulin, Energiya Scientific Production Association; UDC 621.039.52]

[Abstract] A counterflow of vapor and water arises in water reactors in the case of an accident with loss of the heat-transfer agent. Such a situation has been examined in a number of published models but with the introduction of a number of semiempirical assumptions for discriminating from a great many stationary modes that one which is stable. For further clarification and stronger validation this problem has been reexamined using the nonstationary equations of hydrodynamics. The counterflow is examined for an accident situation at a nuclear power plant with a standard reactor when as a result of a rupturing of the discharge line there is a pressure drop in the body of the reactor and levels are formed in the upper and lower mixing chambers. The formation of these levels in turn results in an unstable hovering of the water layer on a vapor cushion. Then the water begins to flow downward under the influence of gravity. The vapor, under the influence of a pressure drop between the upper and lower mixing chambers, flows upward. The flow in the reactor core is simulated by a flow in a vertical channel. The heat-releasing assemblies filling the core zone are simulated by a homogeneous porous medium. Allowance is made for friction-induced pressure losses between each of the flows and core zone structure. An analysis of the equations of hydrodynamics used in connection with this model indicated that the setting-in of a counterflow is accompanied by a wave

process which is similar to the setting-in of critical escape into the atmosphere from a high-pressure vessel. This analogy is further explained. Figures 3; references: 3 Western.

Nonlinear Interaction of Waves During Development of Ionization Instability in Magnetized Nonequilibrium Plasma

937J0107A Moscow TEPLOFIZIKA VYSOKIKH TEMPERATUR in Russian Vol 31 No 3, Mar 93 (manuscript received 21 Dec 92) pp 344-351

[Article by O.A. Sinkevich and V.T. Uklova, Moscow Institute of Energetics; UDC 533.951]

[Abstract] A method of analyzing nonlinear interaction of waves in a magnetized nonequilibrium plasma is proposed, of particular concern being the interaction of ionization waves in an a.c. or compound a.c.-d.c. MHD-generator with a small magnetic Reynolds number. For a demonstration of this method is considered an infinitely long y-channel between two nonconducting walls at $x = 0$ and $x = b$, the limiting case of a channel between two disks with very large radii. All processes are referred to electrons, ions and atoms being treated as given background. Inasmuch as ionization instability develops in a plane perpendicular to the magnetic field vector, the problem is a two-dimensional one. Disregarding the induced magnetic field and radiation, the fundamental system of equations (O.A. Sinkevich, O.S. Popel, V.I. Batov; USSR Patent No 663,942; 1977) is reduced to system of two equations for the electron concentration n and the electric potential Φ. The two orthogonal components of current density j_0 are $j_x = \delta\Phi/\delta y$ and $j_y = j_0 - \delta\Phi/\delta x$ ($j_x = 0$ at both walls). The electron temperature T is assumed to be constant at both walls and the temperature dependence of the electron concentration n to obey Saha's equation, inasmuch as a stable ionization-recombination equilibrium is reached in a time much shorter than the instability development time. The two equations are reduced to dimensionless form, in which the characteristic dimension of thermal conductivity λ and the coefficient with $(T/\delta n)(n/n_0)$ in the energy equation are small. This signifies presence of a thin boundary layer across which the electron temperature changes steeply. Following expansion of $1/\sigma$ and Ω/σ in the field equation (σ- electrical conductivity, Ω- Hall coefficient) into complete fourth-degree polynomials, the system of these two equations is reduced to an infinite with respect to wave numbers system of ordinary differential equation. This system, with appropriate boundary conditions, is solvable on a computer by the Runge-Kutta method with automatic step selection. Calculations were made for an Ar + (0.01-1.0)% Cs plasma (electron temperature T= 2000-6000 K, atom temperature 300-1500 K, pressure 0.5-10 atm), also according to the linear theory. The results indicate that the mode of stability loss depends not on the initial conditions but only on the system parameters: 1) soft loss of stability when all nonlinear terms have negative coefficients, stiff loss of stability when there are positive and negative coefficients. In a subcritical plasma soft loss of stability is attended by decay of all waves. In a supercritical plasma soft loss of stability is attended by interaction of only waves with $K \leq 10$, waves with $K > 10$ quickly decaying so that an almost monochromatic wave with a finite amplitude survives. As the degree of supercriticality increases, the dependence of its amplitude on the Hall coefficient changes from a root-law dependence to a linear one. Stiff loss of stability is shown to be possibly, depending on the plasma conditions, also attended by self-excitated oscillations with a finite amplitude. Figures 7; references 19.

Mathematical Simulation of Radiative Defects in Microelectronic Devices

937J0106A Dubna FIZIKA ELEMENTARNYKH CHASTITS I ATOMNOGO YADRA in Russian Vol 24 No 1, Jan-Feb 93 pp 246-284

[Article by V.S. Barashenkov, A.N. Sosnin, and S.Yu. Shmakov (Joint Institute of Nuclear Research, Dubna), N.G. Goleminov (Moscow Institute of Engineering Physics), A. Polanski (Institute of Problems in Nuclear Physics, Swierk/POLAND); UDC 539.1.043]

[Abstract] Since elements of modern microelectronic devices with a "honeycomb" structure now contain up to or more than 100,000 semiconductor cells and those of still experimental cryogenic devices contain large arrays of high-temperature superconductor films, a problem arises in predicting their failure due to defects caused by cosmic rays during operation in space or by bombardment by particle beams during measurement in accelerators. Satellite data indicate that cosmic rays cause on the average one such failure in 24 h. Not less vulnerable are microstrip-line detectors in which irradiation and bombardment induce leakage currents. For solution of this problem by statistical techniques is proposed a Monte Carlo model of applicable to a wide range of device configurations and specifically to bombardment by protons, neutrons, or ions. The model simulates an internuclear cascade and its algorithm consists of five steps: (1) pick out energy and other parameters of primary particle; (2) check whether particle is pi meson and calculate probability of its decay if it is, (3) calculate flight range if particle has not decayed, (4) calculate parameters of nuclear interaction (characteristics of nascent particles and of residual nucleus or fission fragments, (5) select new particle if first one has decayed return to step (1) if particle was a primary one. The integral equation of flight range between two successive nuclear interactions is solved by the "equalization of cross-sections" method (S.M. Yermakov and G.A. Mikhaylov, 1972). Because experimental data on the cross-sections are scarce, they are described by a theoretical approximation which includes the mass numbers A and charges Z of both incident and target nuclei, the Coulomb barrier for this pair, and a weakly energy-dependent factor different for different nuclei. Nuclear interactions are described by the "cascading-evaporation" model (Barashchenkov and others). In this model inelastic interaction of particles having an energy within the lower part of the 10-100 MeV range is accompanied by formation of a highly excited compound nucleus which will decay with attendant emission of one neutron or two neutrons or one gamma quantum, while interaction of particles having an energy within the upper part of the 10-100 MeV range proceeds in three successive stages: 1) fast "cascading" (emission of new nascent particles and knocked-out intranuclear nucleons), 2) relaxation of the nucleus to equilibrium with or without attendant emission of fast particles, 3) relatively slow "decay" with attendant loss of excitation energy due to competing fission of nucleus and evaporation of particles. For interaction of nucleons having an energy not exceeding 50 GeV, as those present in cosmic rays, there are are also available approximate "quark-gluon string" models. By means of this mathematical apparatus are evaluated the threshold-dependent probabilities and frequencies of energy release, also the energy spectra of energy release, in Si and GaAs thin films upon their interaction with bombarding protons, alpha particles (He nuclei), and multiple-charge ions (^{12}C). The first example is a detector with an 85 μm thick Si or GaAs film, its sensitive region with a 2.5 cm^2 large surface area being bombarded by 3.65 GeV particles: 1) protons, 2) ^{12}C ions, 3) ^{4}He:^{7}Li:^{10}B:^{12}C:^{14}N:^{16}O = 18:11:1:3:6:6:55 mixture of nuclei. More energy is found to be released in a GaAs film than in a Si film, evidently because a thin GaAs film has a larger macroscopic cross-section for interaction with bombarding particles as well as a more developed hadron-meson cascade forming during inelastic nuclear collisions. In a GaAs film, moreover, a proton beam does not fragmentize target nuclei as much as does a beam of heavy ions so that more heavy fragments are left to contribute to the energy-releasing interaction. The second example is a microcircuit, specifically a 10 μm thick Si device consisting of 4000 cells on a Si substrate, failures here due to radiative defects being simulated assuming a 2 MeV threshold energy. The third example is a Si stripline detector, failures in which due to radiative defects are caused by knockout of atoms from the crystal lattice by bombarding particles (specifically a beam of 3.65 GeV carbon ions or 10.5 MeV neutrons). An example of superconducting devices is a cryogenic bolometer, specifically one whose sensing elements are high-temperature superconductor ($YBa_2Cu_3O_{7-d}$) films on a $SrTiO_3$ substrate. Such a bolometer in a copper holder on an alumina base was placed inside a cryostat with an aluminum wall with a silica inlet window for a bombarding beam of $800\ ^{12}C$ ions/(cm^2.s) intensity. Temperature changes caused by such a beam were found to be so much smaller than $\Delta T_c = 1.2$ K as not to noticeably change the sensitivity of this instrument, a 10% change of its sensitivity requiring a temperature change of at least 0.1 K and thus a beam of 10^{17}-$10^{18}\ ^{12}C$ ions/(cm^2.s) intensity (lower intensity of beam of heavier ions). The authors thank L.N. Zaytsev for suggestions and a stimulating critique. Figures 30; tables 6; references 56.

Effect of Diffraction at Reflector Edges on Amplification of Backscatter in a Turbulent Atmosphere

947J0002A Tomsk OPTIKA ATMOSFERY I OKEANA in Russian Vol 6 No 4, Apr 93 (manuscript received 25 Dec 92) pp 3 69-376

[Article by V. A. Banakh, Institute of Atmospheric Optics, Siberian Division, Russian Academy of Sciences, Tomsk; UD C 621.373.626:551.510.5]

[Abstract] It is shown that diffraction at the reflector may have a substantial effect on the dis tribution of the intensity of the reflected wave and the amplification of backscatter when there is weak turbulence. The depend ence of amplification on the Fresnel number of the reflector is oscillatory for a flat or corner specular reflector. The effect of diffraction at the reflector edges on backscatter amplification becomes insignificant in the transition to strong turbulence . The calculations confirm the conclusion that the Gaussian model of the amplitude distribution of the reflection coefficient, without considering reflector edge diffraction, gives correct results for the distribution of intensity of a reflected wave only in extreme cases. For intense turbulence, turbulent distortions of the reflected spherical wave prevail over diffraction effects, and the Gaussian model may be used. This is also the case when the reflector has a diffusely scattering surface. Figures 3; references 21: 17 Russian, 4 Western.

Use of Convex Boolean Programming To Solve the Problem of Optimal Placement of Actuators in Flexible Mirrors

947J0002B Tomsk OPTIKA ATMOSFERY I OKEANA in Russian Vol 6 No 4, Apr 93 (manuscript received 9 Jul 92) pp 392-397

[Article by R. T. Yakupov, V. D. Kuznetsov Siberian Physicotechnical Institute, Tomsk; UDC 535.416.3]

[Abstract] The quality of an adaptive optics system depends on the optimal placement of actuators. Typically, methods yieldi ng approximate solutions to this problem are used. The problem is that it is difficult to determine how far from optimal the so lutions are. This article proposes an approach which yields an exact solution for a given optimality criterion, or an approxima te solution with a guaranteed relative or absolute exactness. The formulation is idealized in that it assumes observation of the phase of the wave front over the entire aperture and the ability to instantaneously correct distortions. One of the equations which is derived can be subjected to convex Boolean programming. There are effective computing algorithms to solve the equatio n which yield not only an exact solution, but the guaranteed approximate solutions noted above. The algorithm is presented. An example is given. Calculations may be done on an IBM PC/AT computer. Tables 2; references 5 (Russian).

Compensation of Nonlinear Distortions of Optical Radiation. Formation of the Wave Front of a Light Beam

947J0002C Tomsk OPTIKA ATMOSFERY I OKEANA in Russian Vol 6 No 4, Apr 93 (manuscript received 6 Oct 92) pp 398-408

[Article by V. A. Trofimov, Moscow State University; UDC 535.416.3]

[Abstract] This article examines the problem of the formation of wave fronts with flexible or segmented mirrors. Results obtained in the study of the selection of mirror geometry (number of degrees of freedom and location of actuators) are presented. The organization of parallel control of various mirror deformation channels is discussed. There is a detailed analysis of the effect of beam intensity profile and the ratio of the actuator range to the beam radius on beam focusing quality. Possible approaches to the modeling of the focusing of optical radiation of a segmented mirror are discussed. Differences from the results obtained in an approximation of the fiel d and those obtained in numerical modeling of wave front inversion in four-wave interaction with strong energy exchange between waves and self-action are noted. Figures 4; table 1; references 41: 37 Russian, 4 Western.

Simulation of Dynamics in Magnetically Squeezed Coaxial Discharge, Part 2: Laws of Two-Dimensional Plasma Flow Formation and Dynamics in Principal Phase

937J0107B Moscow TEPLOFIZIKA VYSOKIKH TEMPERATUR in Russian Vol 31 No 3, Jun 93 (manuscript received 13 Jul 92) pp 357-363

[Article by V.Ye. Okunev, G.S. Romanov, and A.S. Smetannikov, Institute of Heat and Mass Transfer imeni A.V. Lykov, Minsk; UDC 533.9]

[Abstract] Plasma flow in a coaxial radiating cold high-current discharge in an azimuthal clamping magnetic field and an axial electric field is described by four partial differential equations of magnetic radiative gas dynamics, in cylindrical coordinates [r,ψ,z]. The physical model of that flow including several attendant processes: 1) heating and vaporization of the tubular dielectric substrate by intrinsic thermal radiation emitted by the plasma, 2) radiative energy transfer, 3) Joule-effect energy release into the interelectrode gap, 4) interaction of the magnetic field and the electric current flowing in the plasma. Viscosity and heat conduction are disregarded, both negligibly influencing the flow in this kind of discharge. These equations, which contain divergence terms along with time derivatives of plasma properties (density, velocity, energy) and pressure gradients, are supplemented with four equations characterizing the dependence of four variables (pressure P, temperature T, thermal conductivity κ of the plasma, electrical conductivity σ) on both density and specific internal energy of the plasma. The thus closed system is reduced to dimensionless form by normalization of the plasma density to 0.1 g/cm^3, the specific plasma energy to 1 kJ/g, the jet velocity to 1000 m/s, the pressure to 10 MPa, the temperature to 1 eV, the magnetic field intensity to 10 kOe, the electric field intensity to 10 V/cm, the current density to 100 kA/cm^2, the electrical conductivity to 10 kS/cm, the power density to 1 MW/cm^2, the coordinates r to 1 cm and z to 1 cm, the time to 10 μs. The system of equations is then solved numerically in the accordingly two-dimensional approximation, for simulation of the plasma flow through and past the ring electrode inside an evaporating dielectric tube. The equation of energy transfer is solved in both one-group (gray body) and multigroup (10 spectral groups approximations. Figures 6; references 4.

High-Velocity Plasma Jets in Air, Part 1: Dynamics of Pulsating Jet Generated by Cumulative Plasmatron With Conical Geometry

937J0107C Moscow TEPLOFIZIKA VYSOKIKH TEMPERATUR in Russian Vol 31 No 3, Jun 93 (manuscript received 17 Sep 92) pp 364-368

[Article by A.P. Yershov,I.Kh. Imad, I.B. Timofeyev, S.N. Chuvashev, V.M. Shibkov, and U. Yusupaliyev, Moscow State University; UDC 533.92]

[Abstract] Attainment of high-velocity unidirectional plasma flow electrodynamically by means of plasma-dynamic discharges in a transverse magnetic field is considered, such a discharge ensuring direct electric-to-kinetic energy conversion. This however requires a special configuration of the electrodes designed to not only minimize their erosion and erosion of the dielectric components but also prevent widening of the plasma stream as the input energy rises to its maximum. The performance of a cumulative pulsed plasmatron with a conical configuration of electrodes and a plasma-generating dielectric insert is analyzed on the basis of a new model rather than the conventional one which equates a plasma-dynamic discharge to a moving current sheath and thus tolerates a shunting MHD instability with attendant change of the discharge mode from plasma-dynamic to quasi-static plasma flow. In the proposed physical model two coaxial conical electrodes, a solid inner one and a tubular outer one, form a conical annular interelectrode channel. This channel is at the wide end closed by a plasma-generating dielectric washer and merges at the narrow end through a membrane into a straight nozzle. The gas (air) filling this channel is driven by the injected plasma jet into the nozzle for discharge into the atmosphere. Interaction of the forward flowing plasma and the resisting gas results in shock compression of both so that a plasma plunger and a plug form on the respective sides of the interface. Their interaction obeys the law of momentum conservation while the condition of impulse balance is satisfied in the zone through which the plasma plunger accelerates the air plug with a force $F \simeq B(0)\pi r(0)\Delta/\mu(0)$. Here $B(0)=\mu(0)I/2\pi r(0)$ is the mean magnetic induction in the interelectrode space at the washer surface, μ_0 is the magnetic permeability of the medium, I is the discharge current, and r(0),r,(Δ) are key geometrical dimensions characterizing the plasmatron configuration. The discharge current, a function of time t, is assumed to rise according to the power-law relation $I= it^N$. The delay of plasma exit from the plasmatron can be controlled by regulating the density of air ρ_a, the rate of current rise $i= I/t^N$, and the ratio of channel length l(0) to washer radius r(0). Formation and flow a plasma in such a channel with copper walls (high thermal conductivity) are analyzed numerically on the basis of this model with N= 1, i= 20 GA/s, air density 1.3 kg/m^3, l(0):r(0)= 2, and current rise time $t(0) \simeq 30$ μs comparable with half a discharge period. Erosion of the electrodes is assumed to be negligible, but the effect of ascendant erosion is also evaluated. The results of these calculations are compared with the results of measurements and verified by photographs of plasma glow taken with a high-speed camera. Figures 4; references 17.

Attaining High Degrees of Stability in Radial Compression of Plasma Liners

937J0115A Moscow FIZIKA PLAZMY in Russian Vol 19 No 7, Jul 93 (manuscript received 25 May 92, after correction 7 Dec 92) pp 856-865

[Article by S.A. Sorokin and S.A. Chaykovskiy, Institute of High- Current Electronics at Russian Academy of Sciences, Siberian Department; UDC 533.9.07]

[Abstract] An experimental study was made concerning the stability problem in radial compression of hollow cylindrical gas-plasma liners by an initially axial magnetic field with attendant emission of soft x-rays, instabilities being known to distort the liner structure and limit the attainable compression level. Two methods of ensuring maximum degree of stability were tested: 1) use of a helical current return path during the initial compression period, while the liner radius still remains within the same order of magnitude; 2) addition of a second stage. Current pulses of 100 ns duration with a 1.1 MA amplitude for the plasmatron were produced by a SNOP-3 generator. For the current return path was used 24-thread helix with a 45° lead angle consisting of 24 stainless steel bars 2.0 mm in diameter. The helix, inside a Helmholtz coil, was placed around the 20-30 mm in diameter reticulate plasmatron anode. Comparative tests were performed with a straight current return path (0° lead angle). Distortion of the helical magnetic lines of force was prevented by connecting the anode mesh to all helix through L-shaped wires 0.7 mm in diameter. Gas (N_2, Ar, Kr) was injected through a deLaval nozzle having an annular orifice 2 mm wide with a 9 mm median radius. The jet divergence was minimized and the zippering effect (nonsimultaneity of maximum compression along the liner axis) was weakened by orienting the a nozzle at an about 7° angle to the liner axis, which also prevented leakage of the gas through the clearances between helix bars. The second method of compression stabilization was also tested with either a helical or straight current return path, a hollow plasma cylinder of a different gas (second stage) having been inserted inside the original liner plasma cylinder (first stage), in an initially coaxial magnetic field. The outer first stage was accelerated by the azimuthal magnetic field of the current flowing through it from the generator, causing this stage to compress the magnetic field between the two stages and this magnetic field then accelerating the inner second stage. In the experiment with a single liner stage the power of soft x-ray emission pulses, within the 190-288 eV range of quantum energy, was measured with an x-ray vacuum diode (aluminum cathode and 3 μm thick mylar filter). In the experiment with two liner stages the power of soft x-rays emission, with higher than 1 keV quantum energy, was measured with a p-i-n diode (80 μm thick titanium filter for continuous-wave emission by nitrogen plasma liner) and the zippering effect was measured with two such p-i-n diodes (1.5 ns time resolution, 62 μm thick mylar + 1 μm thick aluminum filter for pulsed emission by argon plasma liner). The integral energy in emission pulses was in this experiment was measured with an open foil bolometer. The boundary of the outer second liner stage, emitting visible light while moving, was tracked with an AGAT-SF chronograph. The plasma pinch was in both experiments tracked and photographed by a camera obscura, several such cameras being used for this purpose (magnifications: K= 1,3; aperture diameters: 90 μm, 45 μm, 15 μm; mylar filter 8 μm or 3 μm thick, aluminum filter 0.2 mm thick). The theoretical condition for minimum instability increments are established for a plasma liner having a finite thickness and no mass. Calculations are based on the zero-dimensional model of a plasma with high electrical conductivity and a magnetic field diffusing into it much slower than the characteristic liner compression time, which corresponds to a magnetic Reynolds number much larger than 1. The results of the experiments reveal that: 1) a helical current return path lowers the initial magnetic induction necessary for producing a stable pinch under maximum compression; 2) a liner consisting of two stages with a different gas in each behaves like an x-ray laser with radiation pumping, such as the Na-Ne x-ray laser (J.P. Aruzese, J. Davis; PHYSICS REVIEW A, Vol 31, 1985). The authors thank V.I. Oreshkin for calculating the power of plasma (argon, sodium) columns on the basis of the collision-radiative model. Figures 6; references 9.

Comparing Equilibrium and Stability Parameters of Plasma in Dragon Trap With Arbitrary Ellipticity of Magnetic Surfaces

937J0115B Moscow FIZIKA PLAZMY in Russian Vol 19 No 7, Jul 93 (manuscript received 27 Oct 92) pp 882-893

[Article by A.V. Dobryakov, Russian "Kuryatov Institute" Science Center; UDC 533.931]

[Abstract] A magnetic plasma trap with an axially nonuniform ellipticity of its magnetic surfaces in a transverse magnetic field with a third harmonic present is selected to serve as a model for estimating plasma equilibrium and stability in the Dragon collision-radiative electron lens (V.M. Glagolev et al.: 1. Tenth European Conference on Controlled Fusion and Plasma, Moscow 1991, report E-8; 2. Conference on Plasma Physics and Controlled Nuclear Fusion Research, Baltimore 1982, Nuclear Fusion Supplement Vol 3), into the originally undistorted magnetic configuration being considered insertion of a stabilizer element with a straight magnetic axis in a magnetic field with with both second and third harmonics. In connection with estimation of the limiting values of the beta factor under equilibrium constraint and the beta factor under stability constraint, the possibility of the two beta factors having equal limiting values is examined by first comparing the theoretical expressions for the two beta factors applicable to not longer than three hemitori and thus "short" crels (collision-radiative electron lenses). The limiting value for equilibrium and the limiting value for stability are then obtained estimated on the basis of the plasma shift and with the aid of the Mercier criterion respectively. The next step is selecting a magnetic configuration which will ensure existence of a mean induction B minimum, the choice being a magnetic configuration with a uniform curvature and symmetric with relative to the crel center. The third and last step is establishment of the relation between the two beta factors and subsequent optimization of both under the constraint that they be equal. Here is considered an originally circular crel with an elliptically deformed stabilizer, a specific example being a crel which consists of three uniformly helical

solenoid segments. The author thanks V.M. Glagolev (deceased) for support and stimulation. Figures 5; references 12.

Anomalous Charge and Heat Transfer in Nonisothermal Plasma With Two Kinds of Ions

937J0115C Moscow FIZIKA PLAZMY in Russian Vol 19 No 3, Jul 93 (manuscript received 25 Jun 92, after correction 5 Oct 92) pp 894-902

[Article by V.P. Silin and S.A. Uryupin, Institute of Physics imeni P.N. Lebedev at Russian Academy of Sciences; UDC 533.951]

[Abstract] Charge and heat transfer during development of ion-acoustic turbulence in a magnetically confined nonisothermal plasma consisting of hot electrons and "cold" ions is analyzed, considering that impurity ions with a different charge-to-mass ratio usually present in the confinement region appreciably influence the properties of a plasma and appreciably raise the probability of induced scattering of ion-acoustic waves by ions in the field of ion-acoustic beats. The analysis is based on the Tsytovich- Pustovalov-Silin theory of a turbulent plasma and takes into account separation of ion charges in a two-component plasma, which gives rise to a new spectrum of ion-acoustic waves and to new anomalous plasma properties. From the expression for the nonlinear sound attenuation according to that theory and assuming a Maxwell distribution of ions, there are derived expressions for both electronic charge and electronic heat fluxes. An expression is also obtained for the effective electron-electron collision frequency less dependent on the degree of plasma nonisothermality in a plasma with two kinds of ions than according to the analogous Sagdeyev's formula (R.Z. Sagdeyev; 1967 SYMPOSIUM ON APPLIED MATHEMATICS, PROCEEDINGS Vol 18) for a plasma with only one kind of ions. References 17.

Emission of X-Ray Pulse Trains by Multiply-Charged Z-Pinch Plasma

937J0115D Moscow FIZIKA PLAZMY in Russian Vol 19 No 7, Jul 93 (manuscript received 21 Dec 92) pp 937-939

[Article by B.N. Mironov, Troitsk Institute of Innovative and Thermonuclear Research; UDC 533.952]

[Abstract] Initiation of plasma instability and its maintenance throughout the rather long discharge period were explored experimentally, the main object being to find ways to increase the x-ray emission yield. Experiments were performed with a noninductive vacuum spark in an iron plasma, the current flowing in the direction of the z-pinch axis reaching the 200 kA level after a 1.25 μs rise time. Radiation emission was recorded by a silicon x-ray detector (time resolution 1.5 ns) and by a high-speed optoelectronic x-ray camera (time resolution 20 ps) with a slotted photocathode. A diaphragm with a 150 μm wide and 10 μm long slit was placed between the camera and the radiation source. The geometry of the measurements was designed that the z-pinch axis run parallel to the slit in the diaphragm and normally to the photocathode of the camera. The slit was covered by a 4 μm thick dacron filter with a 0.3 μm aluminum coating. Further experimentation resulted in successful formation of various numbers of plasma clusters with x-ray emission characteristics approaching those of micropinches. A comparison of the oscillograms of x-ray pulses emitted by a plasma containing 2, 3, 4, ... inhomogeneities with the oscillogram of x-ray pulses emitted by a classical micropinch indicates that it is feasible to lengthen the duration and increase the integral yield of x-ray emission at a given discharge current level, formation of a plasma capable of emitting trains of x-ray pulses depending principally on both shape and size of the anodic discharge region. The author thanks V.V. Gavrilov for support, also S.V. Ilina, O.L. Ledova, and T.N. Buryakova for help with processing and documenting the results. Figures 2; references 2.

Current Fluctuations in Superconductor With Superlattice in Strong Electric and Magnetic Fields

937J0099A St. Petersburg FIZIKA TVERDOGO TELA in Russian Vol 34 No 8, Aug 92 (manuscript received 13 Sep 91) pp 2326-2336

[Article by A. D. Margulis and Vl. A. Margulis, Mordovian State University imeni N. P. Ogarev, Saransk; UDC 539.21]

[Abstract] In superconductors with a superlattice placed in external fields there are a number of specific effects absent in ordinary superconductors. They may be of considerable practical interest, but the literature contains virtually no pertinent information. A study was therefore made of spatially uniform current fluctuations in a semiconductor superlattice exposed in classically strong constant electric and magnetic fields. It was assumed that the electric field E is directed along the superlattice axis and the magnetic field H has components both parallel and perpendicular to this axis. Such an orientation of the fields is important because it can cause resonance of the static current when there is a coincidence of multiple Stark and cyclotron frequencies (Stark-cyclotron resonance). The analysis of research on this phenomenon is summarized and a series of figures shows the spectral dependence of current fluctuations in a superlattice in strong electric and magnetic fields; dependence of spectral density of current fluctuations at the low-frequency limit on the electric field and superlattice volt-ampere characteristic; spectral density of current fluctuations at the low-frequency limit on the magnetic field and superlattice gauss-ampere characteristic. Figures 3; references 18: 15 Russian, 3 Western.

Influence of Strong Electric Field on Conductivity of High-Temperature Superconductor Ceramic of YBaCuO System

937J0099B St. Petersburg FIZIKA TVERDOGO TELA in Russian Vol 34 No 8, Aug 92 (manuscript received 12 Mar 92) pp 2482-2486

[Article by B. I. Smirnov, S. V. Krishtopov and T. S. Orlova, Physical Technical Institute imeni A. F. Ioffe, Russian Academy of Sciences, St. Petersburg; UDC 537.312.62]

[Abstract] A study was made of the change in conductivity of high- temperature superconducting (HTSC) ceramic of the $YBa_2Cu_3O_{7-x}$ system in an electrode-dielectric-superconductor system directly under the influence of constant electrostatic fields of different polarity with a strength up to 140 MV/m which were imparted to the sample when $T < T_c$, in this particular case 77 K. A second ceramic to which 8% Ag had been added also was investigated. It had already been established that in HTSC materials under the influence of an electrostatic field or after processing by an electric field there may be a change in both the critical temperature T_c and the critical current I_c. The analytic results are represented in the form of volt-ampere characteristics. It was established that with a temperature $T < T_c$ an external constant electrostatic field exerts an influence on the conductivity of HTSC ceramic when $I > I_c$ and may lead to both an I_c decrease and increase. The addition of Ag exerted a significant influence. The observed effects are attributable to the redistribution of the carriers (holes) in the sample under the influence of the imparted field. Figures 6; references 8: 7 Russian, 1 Western.

Nonphonon Superconductivity of Cubic Monocarbides and Mononitrides

937J0099C St. Petersburg FIZIKA TVERDOGO TELA in Russian Vol 34 No 8, Aug 92 (manuscript received 17 Mar 92) pp 2522-2528

[Article by P. O. Zaytsev and Yu. V. Mikhaylova, Atomic Energy Institute imeni I. V. Kurchatov, Moscow]

[Abstract] A study was made of the phase diagram of MC and MN compounds with a B1 structure (whose properties are characterized by n_p and $n_d = 4$ and 5). The compound ScC, for which $n_p + n_d = 7$, also is examined. It appears that a nonphonon superconductivity mechanism is possible, as is the case for cuprate HTSC. Within the framework of a very simple Emery model it was possible to determine the electron structure of elementary excitations and also their partial scattering amplitudes relating to the Fermi level. An approximate expression is derived for the Bardeen-Cooper-Schrieffer constants by means of which it is possible to find the regions of existence of a superconducting state, which makes possible a comparison with experimental data. The existence of superconductivity with adequately high T_c for the group of compounds with $n_p + n_d = 4$ and 5 can be explained using a representation of the negative amplitude of d-d scattering in the lower hole subzone. The absence of superconductivity in the case $n_p + n_d = 6$ is attributable to the fact that for this family the Fermi level passes within the hybridization gap. The compound ScC passes into a superconducting state due to the negative amplitude of p-p scattering. The realization of superconductivity in the case $n_p + n_d = 3$ is possible only due to interaction through phonons. Figures 2; references 8: 5 Russian, 3 Western.

Size-Dependent Indirect Exchange, Magnetoelectric Effect and Superconductivity in Small Particles and Thin Films

937J0103A Moscow PISMA V ZHURNAL EKSPERIMENTALNOY I TEORETICHESKOY FIZIKI in Russian Vol 57 No 5-6, Mar 93 (manuscript received 18 Feb 93) pp 360-362

[Article by E. L. Nagayev, High-Pressure Physics Institute, Russian Academy of Sciences]

[Abstract] A study was made of indirect exchange in magnetic samples of finite size. It is shown that two factors are responsible for the dependence of indirect exchange on size: appearance in the effective exchange integral of a term associated with the surface and a change in the volume term due to the dependence of Fermi momentum on size. Both these factors are essentially dependent on the boundary conditions for electrons at the sample surface. They can be changed by adsorption or an external electric field. Accordingly there will be a change in the type of magnetic ordering or its quantitative parameters and it is possible to postulate a new form of magnetoelectric effect: a surface magnetoelectric effect. An interesting effect is associated with the dependence of indirect exchange on size: whereas Gd clusters of a definite size behave normally, as superparamagnetic particles, Gd clusters of other sizes behave anomalously, being deflected in the direction of weak fields in a Shtern-Gerlach apparatus. Since clusters of the weak magnetics V, Pd, Al and even the strong magnetic Cr are not deflected at all, it can be concluded that anomalous Gd clusters are strongly diamagnetic, which may be a consequence of their superconducting state. This seems to contradict the fact that Gd is a ferromagnetic metal and superconductivity is therefore forbidden in it. However, due to the dependence of indirect exchange on size small Gd clusters are not necessarily ferromagnetic and therefore superconductivity in them is not forbidden. It therefore appears that the indirect exchange integral in small magnetic particles and in thin films is dependent on their size. Whereas in massive samples indirect exchange establishes ferromagnetic ordering, small particles may become antiferromagnetic and superconducting. References: 4 Western.

Study of Pinning in High-Temperature Superconductors

937J0110A Moscow ZHURNAL EKSPERIMENTALNOY I TEORETICHESKOY FIZIKI in Russian Vol 104 No 1(7), Jul 93 (manuscript received 23 Feb 93) pp 2519-2525

[Article by V. N. Bakradze, A. A. Iashvili, T. V. Machaidze, T. K. Nakhutsrishvili, Dzh. G. Ch igvinadze, Institute of Physics, Georgian Academy of Sciences]

[Abstract] The effect of vortex pinning is studied in the superconducting ceramic YBaCuO using a mechanical method. The samples had a superconductivity transition temperature around 94 K . The experiments were conducted at the temperature of liquid nitrogen (77.3 K). Torque is generated in samples rotating in a homogeneous magnetic field. This torque is associated with the presence of pinning of a vortex magnetic structure. The pinning force, $F_p = 3X10^{-5}$dyne/cm (in a 1 kOe field) is determined from the torque. There is a linear dependence of torque on the rate of rotation of the sample at high rotation speeds. At lower speeds torque decreases snarply . This is because at high speeds vortex movement occurs in a flux flow mode, and at low speeds it occurs in a flux creep mode. Torque relaxation which was logarithmic over time was observed at the temperature of liquid nitrogen. A model is proposed which, based on the theory of thermoactivation flux creep (Anderson's theory), explains these phenomena. The pinning potential was found to be $U_0 \approx 250$ MeV. Figures 7; table 1; references 13: 2 Russian, 11 Western.

On Nonlocal Josephson Electrodynamics

937J0110B Moscow ZHURNAL EKSPERIMENTALNOY I TEORETICHESKOY FIZIKI in Russian Vol 104 No 1(7), Jul 93 (manuscript received 2 Mar 93) pp 2526-2537

[Article by Yu. M. Aliyev, V. P. Silin, Lebedev Physics Institute, Russian Academy of Sciences]

[Abstract] Results of previous publications on Josephson electrodynamics are summarized. Nonlocal Josephson electrodynamics has not been developed extensively because the theory is incomplete. The formulas needed to describe the magnetic field of vortices, their energy, and the Lagrangian and Hamiltonian functions of unstable vortices (fluxons) are developed for the tunnel junction between two different superconductors. A general relation is found which defines the magnetic field in superconductors using the difference in Cooper pair phases. At the asymptotic nonlocal limit, a solution is obtained for a travelling kink with a constant speed, which, in contrast to the travelling kink of local theory, has two quanta of magnetic flux. This solution is the first description of a moving regular Abrikosov vortex. References 6: 4 Russian, 2 Western.

Dynamic Conductivity and a Coherent Peak in the Submillimeter Spectra of NbN Superconducting Films

937J0110C Moscow ZHURNAL EKSPERIMENTALNOY I TEORETICHES KOY FIZIKI in Russian Vol 104 No 1(7), Jul 93 (manuscript received 12 Mar 93) pp 2546-2555

[Article by A. A. Volkov, B. P. Gorshunov, I. V. Fedorov, A. D. Semenov, Institute of General Physics, Russian Academy of Sciences]

[Abstract] NbN is one of the popular low-temperature superconductors, but there is virtually no experimental data on NbN absorption and dielectric properties in the submillimeter range. This article develops a method to measure the electrodynamic parameters of superconducting films in the submillimeter range, and to systematically measure the submillimeter spectra of dynamic conductivity and permittivity of NbN superconducting films. The method is based on the use of a Fabry-Perot interfeometer formed by two films applied from both sides on a dielectric substrate. At frequencies of 5-39 cm^{-1} and at temperatures of 5-300 K the first detailed measurements are made of the dependences of dynamic conductivity and permittivity of superconducting NbN

films on temperature and frequency. A coherent peak is recorded for the first time in the dependence of dynamic conductivity on temperature. The coherent peak indicates the singlet nature of the ground state of this compound. Figures 6; references 14: 8 Russian, 6 Western.

Study of the Anharmonics of Vibrations of Cu and O Atoms in an Y Ceramic Using Inelastic Neutron Scattering

937J0111 St. Petersburg FIZIKA TVERDOGO TELA in Russian Vol 35 No 2, Feb 9 3 (manuscript received 14 Jul 92) pp 310-319

[Article by V. K. Fedotov, A. I. Kolesnikov, V. I. Kulakov, Ye. G. Ponyatovski y, I. Natkanets, Ya. Mayer, Ya. Kravchuk, Institute of Solid State Physics, Russian Academy of Sciences, Chernogolovka; UDC 538. 91+539.27+537.312]

[Abstract] The results of previous publications dealing with the behavior of high-temperature superconductors, in particular, YBCO, are discussed. Inelastic neutron scattering in an incoherent approximation is used, as well as isotopic contrasting, to determine the partial contributions of vibrations of Cu and O atoms to the density of phonon states in YBC O. The temperature behavior of the spectra was used to detect the anharmonics of O atoms in the rhombic phase. The nature of the anharmonics and the dynamic values of the thermal factor and the Debye temperature are discussed. A generalized spectrum of vibrations is obtained. The one-phonon generalized phonon state density is calculated after the contribution of multi-phonon neutron scattering is subtracted. The partial spectrum of vibrations of Cu atoms in the superconducting rhombic phase and the tetragonal phase of YBCO is calculated at temperatures of 80 K and 290 K. A weighted partial density of vibrations of O atoms is obtained for the same temperatures. In the isotopic approximation, no anharmonism was detected in the vibrations of Cu atoms. The data obtained here do not confirm the presence of a local two-well potential in the oxygen positions; however, the data indicate a strong interaction of optical phonons and other collective excitations of the high-temperature superconductor. Figures 5; references 49: 8 Russian, 41 Western.

Plasma Excitations in Low-Dimensional Systems

937J0111J St. Petersburg FIZIKA TVERDOGO TE LA in Russian Vol 35 No 2, Feb 93 (manuscript received 16 Jul 92) pp 324-329

[Article by Ye. A. Andryushin, A. P. Silin, Le bedev Physics Institute, Russian Academy of Sciences, Moscow]

[Abstract] In low-dimensional systems, which are modelled here by a set of planes and threads along which free electrons move, the dynamic permittivity of the system is defined as Coulomb interaction between electrons from different planes and threads. If the distance between planes or threads is less than the effective Bohr radius, the Coulomb interaction can be approximated by chaotic phases. Explicit expressions are obtained for the dispersion law of plasmons for a number of models of low-dimensional systems. It is found that consideration of the anisotropy of motion and the spatial distribution of charges in all cases leads to acoustic dispersion of the plasmon, as well as most plasmon branches. In the one- and two-dimensional cases, a consideration of the interaction of threads and layers respectively leads to acoustic dispersion of plasmons in virtually the entire plasmon zone, except at the boundaries. The interaction of electrons and acoustic plasmons may increase the critical temperature of the superconductor with a phonon superconductivity mechanism. References 29: 8 Russian, 21 Western.

Low-Temperature Thermodynamics of Magnetically Ordered Narrow-Band States in Hubbard-Type Magnetic Material

937J0112E Kharkov FIZIKA NIZKIKH TEMPERATUR in Russian Vol 19 No 3, Mar 93 (manuscript received 21 Sep 92, after revision 25 Nov 92) pp 274-283

[Article by E.Ye. Zubov, Donetsk Institute of Engineering Physics at Ukrainian Academy of Sciences; UDC 538.22]

[Abstract] A narrow-band magnetic material is considered in connection with high-temperature superconductivity of metal-oxide materials such as ($RBa_2Cu_3O_{6+d}$ (R=Y,Nd,Sm) compounds and the role which magnetic degrees of freedom play in electron pairing. Such a material is described by the Hubbard t-J model of a close-correlated system with a kinetic energy U of intra-atomic Coulomb repulsion much higher than the energy t of internodal electronic transitions. According to this model, in such a material the ground state of the lattice of 3d-ions in the partly occupied band is an antiferromagnetic (Ne'el) state. According to Nagaoka's theorem, moreover, inclusion of one hole in plain cubic and body-centered cubic lattices with infinitely strong Coulomb repulsion causes decay of the antiferromagnetic state and formation of a stable saturated ferromagnetic one. Formation of such a state as well as generally the effect of exchange interaction, doping level, and thermal fluctuations on the ground state structure are analyzed by a statistical method which uses the scattering matrix formalism, graphical summation being used for calculating the thermodynamic functions. Into account is taken the possibility of a two-sublattice structure formed by an effective self-consistent field when exchange interactions take place, and the 3d-electrons in the Cu subsystem are assumed to occupy the lower Hubbard band. On this basis is formulated the Hamiltonian of such a system and is calculated the effective interaction. A system of equations for the components of both magnetization and chemical potential, also for the free energy,

is derived in the nonvanishing first approximation with respect to the small parameter t (kinetic energy of internodal electronic transitions). This system is solved for three simplest cases: 1) homogeneous antiferromagnetic phase, 2) homogeneous ferromagnetic phase, 3) paramagnetic phase. An analysis of the results indicates that at sufficiently low ($T/W << 1$ (T- temperature, W-width of energy band) the magnetization density decreases down to zero, this being the effect of thermal fluctuations on the saturated ferromagnetic ground state. At zero temperature doping with oxygen causes most holes to migrate into ferromagnetic clusters. At temperatures above zero the lattice magnetization drops to zero at some dopant concentration, which signifies decay of the Nagaoka state and a smaller effective kinematic contribution to the free energy. The authors thank Yu.A. Dimashko for discussion. Figures 7; references 17.

Effect of Electron Bombardment on Peak-Effect in $YBa_2 Cu_3O_x$ Single Crystals

937J0112A Kharkov FIZIKA NIZKIKH TEMPERATUR in Russian Vol 19 No 3, Mar 93 (manuscript received 17 Jul 92, after revision 8 Oct 92) pp 244-248

[Article by T.I. Arbuzova, I.B. Smolyak, V.L. Arbuzov, A.E. Davletshin, S.V. Naumov, and A.A. Samokhvalov, Institute of Metal Physics at Russian Academy of Sciences (Ural Department), V. Gavalek, Institute of Engineering Physics, Jena/GERMANY; UDC 538.945]

[Abstract] An experimental study was made concerning the effect of electron bombardment on the superconducting transition of $YBa_2 Cu_3O_x$ single crystals and the role of defects in the peak-effect. The experiment was performed with two differently grown single crystals: (A) thin lustrous plate weighing 1.5 mg grown from solution in a melt, its superconducting transition being precipitous with a critical temperature 92+/-0.1 K; (B) thicker plate weighing 20 mg grown by the quench mount method, its superconducting transition being soft with a critical temperature 86+/24 K). The parameters of their crystal lattices were measured under a DRON-2.0 x-ray diffractometer with a CrK_α- radiation source. They were bombarded with 5 MeV electrons at a 250 K temperature in a helium channel cryostat, the fluence being varied stepwise over the $5x10^{18}$-$2.2x10^{19}$ cm^{-2} range for crystal A and over the 10^{18}-$2x10^{19}$ cm^{-2} for crystal B. Changes of the critical temperature were then monitored by inductance measurements in magnetic fields of lower than 0.1 Oe intensity and with a resistance thermometer. For all measurements the specimens were reheated to room temperature after each bombardment. Magnetization curves covering the 0-15 kOe range of field intensity were recorded in a vibration magnetometer at 77 K, the peak-effect having been found earlier to be most pronounced at temperatures close to the critical. Magnetization of crystal B was found to be characterized by a normal hysteresis loop and magnetization of crystal A by an anomalous one, one with a second peak within the intermediate range of magnetic field intensity. The critical current for both specimens determined initially and after each bombardment, the magnetic induction being varied of over the 0-1.5 T range. While increasing the bombardment dose lowered the critical current for crystal B monotonically throughout the entire range of magnetic induction, it changed the critical current for crystal A differently: its dependence on both the bombardment dose and the magnetic field being more intricate. Increasing the bombardment dose evidently weakened the peak-effect in crystal A. This is interpreted as a result of a magnetic vortex becoming eventually larger than a radiative defect so that the latter ceases to be an effective pinning center. Various pinning mechanisms possibly leading to the peak-effect are examined, the most likely one being a change of energy of supercurrent-vortex interaction at the boundary between two superconducting phases. Figures 3; tables 1; references 7.

Nonequilibrium Processes in $YBa_2Cu_3O_{7-d}$ Superconducting Ceramic Stimulated by Electromagnetic Microwave Field and by Direct Current Higher Than Critical

937J0112B Kharkov FIZIKA NIZKIKH TEMPERATUR in Russian Vol 19 No 3, Mar 93 (manuscript received 2 Oct 92, after revision 10 Nov 92) pp 249-255

[Article by V.M. Dmitriyev, I.V. Zolochevskiy, and Ye.V. Khristenko, Institute of Low-Temperature Engineering Physics imeni B.I. Verkin at Ukrainian Academy of Sciences, Kharkov; UDC 538.945]

[Abstract] An experimental study of $YBa_2Cu_3 O_{7-d}$ superconducting ceramic was made concerning nonequilbrium processes stimulated in this material by an external electromagnetic microwave field and by a direct current higher than critical, either of them giving rise to an unbalance between the populations within both electron- like and hole-like branches of the quasiparticle energy spectrum. Tests were performed on a 5 mm long bar 1 mm^2 in cross-section cut from an almost purely 123-phase $YBa_2Cu_3O_{7-d}$ ceramic with a less than 10% "green" phase impurity and a critical superconducting transition temperature T_c= 93 K. This bar was tested three times, after a 1.1 mm long middle segment of it had been successively reduced to: 1) a 0.7x0.4 mm^2 bridge for the first test, 2) a 0.5x0.3 mm^2 bridge for the second test, 3) a 0.4x0.3 mm^2 bridge for the third test. The bar was each time placed inside a rectangular waveguide parallel to the electric component of the electromagnetic field for measurement of its current-voltage characteristics up to 10 mV with a direct current, the frequency of the microwave electromagnetic field being varied over the 12-37 GHz range and the ambient temperature T being varied from 3.7 K to 65 K. The temperature dependence of the critical current followed each time the $I_c = k(T_c - T)^{3/2}$ relation, as does the Ginzburg-Landau unpairing current. The microwave power P was stepwise attenuated from the critical level (zero critical current) down to zero. These measurements revealed how the

current-voltage characteristic, the critical current I_c, the excess current $I - I_{R=0}$, and the superconducting transition current I_{N-S} depend on the incident microwave power. The electromagnetic field was found to identically influence the behavior of all three bridges. The results of the experiment indicate that two nonequilibrium processes besides Josephson tunneling take place in high-temperature superconductors just as they do in low-temperature ones such as Sn-13 and Nb-Sn. One of them is supercurrent stimulation by an electromagnetic field in accordance with the Aslamazov-Larkin mechanism (ZHURNAL EKSPERIMENTALNOY I TEORETICHESKOY FIZIKI Vol 74, 1978), owing to "jitter" of the potential well in the bridge region and consequently higher energy of electrons localized in it. Another such nonequilibrium process is formation of phase slip centers by an either direct or high-frequency current higher than critical. Three such centers had been evidently formed one after the other in the thinnest bridge (0.4x0.3 mm^2), as indicated by three successive slightly upward sloping voltage steps within the 0-10 mV range of its current-voltage curves and attendant discrete changes of its electrical resistance. Further measurements have revealed that both their dynamic resistance and zero-voltage "cutoff" current increase linearly with decreasing temperature. Figures 10; references 20.

Phenomenological Theory of Two-Band Crystalline Superconductors With Tetragonal or Orthorhombic Symmetry

937J0112C Kharkov FIZIKA NIZKIKH TEMPERATUR in Russian Vol 19 No 3, Mar 93 (manuscript received 16 Nov 92) pp 256-267

[Article by Yu.M. Poluektov, Kharkov Institute of Engineering Physics; UDC 538.94]

[Abstract] The phenomenological Ginzburg-Landau theory is applied to crystalline superconductors with two overlapping conduction bands and either tetragonal (D_{4h} point group) or orthorhombic (D_{2h} point group) symmetry, this class including heavy-fermion superconductors and probably also high-temperature ones. The number of components the order parameter has is determined by both the number of overlapping bands and the dimensionality of the irreducible representation according to which the superconducting transition proceeds. The number of components the order parameter associated with tetragonal two-band superconductors can have is one or two or three, because the D_{4h} point group has eight one-dimensional and two two-dimensional irreducible representations. The order parameter associated with orthorhombic two-band superconductors can be only one which has two components, because the D_{2h} point group has only eight one-dimensional irreducible representations. The basis functions in these irreducible representations are, for the case of singlet pairing, constructed from products of wave vector projections (the number of projections being an even one) with the aid of either the projection operator or the Clebsch-Gordan coefficients. The volume density of the thermodynamic potential density φ in vicinity of the critical temperature is obtained accordingly in all representations, this potential depending on both pressure P and temperature T, on the order parameter and the space derivatives of its components, and on the vector potential A. Minimizing φ by integrating it over the superconductor volume and then equating to zero the variation of the total thermodynamic potential Φ with respect to components of the order parameter (disregarding its surface components) yields the Ginzburg-Landau equation in each representation. Variation of the total thermodynamic potential Φ with respect to the vector potential A yields the Maxwell equation curl H= $4\pi j/c$ (H- magnetic field) and for the supercurrent density the relation $j = -c\delta\varphi/\delta A$. Further calculations in accordance with this theory for two-band superconductors yield expressions for the critical tetragonal-to-orthorhombic and superconducting transition temperatures. Tables 4; references 22.

Increase of Conductivity of Ceramic High-Temperature Superconductors Prior to N — S Transition

937J0112D Kharkov FIZIKA NIZKIKH TEMPERATUR in Russian Vol 19 No 3, Mar 93 (manuscript received 26 No 91) pp 268-273

[Article by V.M. Dmitriyev, M.N. Ofitserov, and N.N. Prentslau, Institute of Low-Temperature Engineering Physics imeni B.I. Verkin at Ukrainian Academy of Sciences, Kharkov, K. Rogacki, Research Institute of Low Temperatures and Structure imienia W. Trzebiatowski at Polish Academy of Sciences, Wroclaw/ POLAND; UDC 537.311.6:538.45]

[Abstract] An experimental study of high-temperature superconductor ceramics was made concerning the increase of their electrical conductivity already at temperatures far above T_c. The experiment was performed with specimens of: Y-Ba-Cu-O ceramic ($YBa_2Cu_3O_x$, T_c= 86-92 K); Y(Sc)-Ba-Cu-O ceramic ($Y_{0.85}Sc_{0.15}Ba_2Cu_3O_x$, T_c= 90-100 K); Y-Ba-Cu(Ti)-O ceramic ($YBa_2Cu_{2.8}Ti_{0.2}O_x$ and $YBa_2Cu_{2.5}Ti_{0.5}O_x$, T_c= 90.5 K); Tl-Ca-Ba-Cu-O ceramic ($TlCa_2Ba_3Cu_4O_x$ and $Tl_2Ba_2Ca_2Cu_3O_x$, T_c= 122-123 K); Bi-Sr-Ca-Cu-O ceramic ($Bi_{2.16}Sr_{1.33}Ca_{0.556}CuO_x$, T_c= 87 K); Sm-Ba-Cu-O ceramic ($Sm_{1.05}Ba_{1.95}Cu_3O_x$, T_c= 94 K. The d.c. conductance was measured by the voltage-current method. The a.c. conductance at frequencies from 100 kHz to 25 MHz was determined on the basis of impedance measurements by the resonance method at temperatures from below 86 K to above 123 K, the specimen inside the cavity being placed within the region of maximum magnetic induction. The impedance was determined from the change of Q-factor and the shift of resonance frequency. The critical superconducting transition temperature T_c was determined on the basis of inductance measurements in a constant magnetic field of a solenoid, varied over the 0-100 Oe range, and also with the specimen levitating in the magnetic field of a permanent magnet. The results of these measurements reveal an anomalous temperature dependence of the resistance

(ohmic loss) R_s and the frequency shift Δf below 190 K prior to N — S transition. This deviation from their normal temperature dependence could be caused by: 1) fluctuation superconductivity, 2) superconductivity within isolated CuO_2 planes, 3) anomalous scattering of electrons by localized magnetic moments, 4) ordering of the oxygen. An analysis of the data indicates that the temperature range of superconducting transition for some of these ceramics consist of two intervals separated by a temperature below which down to T_c a magnetic field influences the resistance and levitation takes place in a constant magnetic field. Above that temperature up to about 200 K a magnetic field does not influence the resistance and levitation in a constant magnetic field does not take place, despite the anomalous increase of conductivity. The authors thank V.I. Shnyrkov, doctor of physical and mathematical sciences, for helpful discussions. Figures 6; references 21.

New Composite Conducting Material: Conducting Concrete (BETEL)

937J0100A Novosibirsk SIBIRSKIY FIZIKO-TEKHNICHESKIY ZHURNAL in Russian No 6, Nov-Dec 92 (manuscript received 20 Aug 91) pp 59-63

[Article by V. Ye. Nakoryakov, G. A. Pugachev and Ye. K. Mayevskiy, Thermal Physics Institute, Siberian Department, Russian Academy of Sciences, Novosibirsk; UDC 621.315.56]

[Abstract] The background for the discussed subject matter can be found in a book by G. A. Pugachev (edited by V. Ye. Nakoryakov) entitled: Tekhnologiya Proizvodstva Izdeliy Iz Elektroprovodnykh Betonov (Technology for the Production of Objects From Conducting Concretes), Novosibirsk, 1988. The Russian term "betel" has been assigned to this conducting concrete, which can be used successfully in replacing costly high-resistance alloys. The list of applications of this material is extensive, including construction elements of various types, such as floors and walls, in heating systems for civilian, agricultural and industrial structures. Some of the special terminology applicable to "betel" is explained. In simple terms it is a composite material based on a cement binder to which finely dispersed ground materials containing carbon is added. It may also contain sand, gravel, and rubble as fillers. The special requirements imposed on "betel" as a conductor of an electric current are outlined. The carbon used must be of a constant quality and granulometric composition. All other conditions being equal, its conductivity will be determined by the carbon content. The fillers used make it possible to vary the properties of this concrete. A series of problems is examined, such as the stabilization of electrophysical properties and determination of mechanical strength. Any change in the volumetric content of the conducting phase results in a change in both the electric and physicomechanical characteristics. Different production technologies, such as vibration, tamping and pressing, are discussed. Research is continuing for betterment of the products. The technical specifications for one variant of the product are given and special applications are listed. References: 3 Russian.

Conducting Concrete: Its Structure and Mechanical Properties

937J0100B Novosibirsk SIBIRSKIY FIZIKO-TEKHNICHESKIY ZHURNAL in Russian No 6, Nov-Dec 92 (manuscript received 20 Aug 91) pp 64-70

[Article by V. Ye. Nakoryakov, G. A. Pugachev and Ye. K. Mayevskiy, Thermal Physics Institute, Siberian Department, Russian Academy of Sciences, Novosibirsk; UDC 621.315.56]

[Abstract] Some structural and mechanical properties of "betel" (conducting concrete) are analyzed. As a multicomponent material the forming of the structure of "betel" begins with the mixing of the dry components (cement and carbon). One of the mandatory requirements on "betel" structure is that there must be direct contact among the carbon particles. The structure of the dry mixture can be represented by a model in which the particles of the components form regular packings of different density. The structural characteristics of the dry cement-carbon mixture are examined on the basis of the theory of packing and using an ideal model of a structure of particles of spherical configuration and identical size for each of the phases. Experiments were carried out and the data were compared with the theoretical results. The tests included those to ascertain the mechanical failure of the concrete. Particular attention was given to tests of the influence of heating on the properties of "betel" (in "betel" objects heat is uniformly released through the entire mass of the material). For example, the cubic strength is not reduced with brief heating to 95°C, but in the cooling process there is an insignificant (about 3%) strength decrease. Samples (cubes and prisms) from the same consignment were subjected to prolonged heating. After prolonged heating for 2 months the breaking point with the compression of cooled cubic samples averaged 70.2 kg/cm^2 (strength was reduced by 10%). A table of correction factors which must be introduced under various heating conditions is given. References: 8 Russian.

Electromagnetic Launch Track Configurations

937J0107H Moscow TEPLOFIZIKA VYSOKIKH TEMPERATUR in Russian Vol 31 No 3, Jun 93 (manuscript received 6 Jul 92) pp 462-475

[Article by O.V. Fatyanov, V.Ye. Ostashev, A.N. Lopyrev, and A.V. Ulyanov, Institute of High Temperatures at Russian Academy of Sciences; UDC 533.9+621.313]

[Abstract] Electromagnetic boosting of large objects on launch tracks to superhigh velocities is examined, the first requirement being to ensure adequate mechanical and electrical strength along with thermal stability of the electromagnetic-to-kinetic energy converter in the acccelaration channel. The second requirement is placement of the sliding high-current contactor on the rails (electrodes) so as to ensure matching of the track with the voltage supply at high armature velocities. The cause of mismatch in a magnetoplasma booster, for instance, is decay of the armature plasma with attendant formation of parasitic current channels shunting the main discharge in front of the moving body and behind the armature. All standard schemes and proposed modifications may be classified according to: 1) kind of propelled armature (metal armature with special contact hardware, plasma armature, hybrid armature with solid core and plasma contactor); 2) mode of excitation by the accelerating magnetic field (self-excitation by the magnetic field of the armature current alone as in a standard shunt motor or additionally by the magnetic field of the current in a series winding as in a compound motor, or separate excitation); 3) mode of current feed to the electrodes (concentrated or distributed). Three schemes of armature and field connection are examined, an

analysis of the voltage-current relations in each scheme in accordance with circuit theory revealing its advantages and drawbacks. Cophasal "forward" current feed or antiphasal "reverse" current feed realized, respectively, by connecting the voltage supply to the rails at the entrance terminals or at the exit terminals of the launch channel, both schemes being applicable to separate excitation and compound self-excitation. Combination cophasal and antiphasal current feed to the armature is obviously a bilateral current feed realizable for both self-excitation and separate excitation. The authors thank Ye.F. Lebedev and V.Ye. Fortov for discussing the results of this analysis. Figures 5; references 34.

Models of Operation of Explosive-Actuated Magnetos With Interception of Magnetic Flux

937J0107I Moscow TEPLOFIZIKA VYSOKIKH TEMPERATUR in Russian Vol 31 No 3, Jun 93 (manuscript received 6 Jul 92) pp 469-475

[Article by V.B. Mintsev, A.Ye. Ushnurtsev, and V.Ye. Fortov, Institute of Chemical Physics, Chernogolovka; UDC 621.37.373]

[Abstract] The performance of multistage explosive-actuated magnetos, economical as well as reliable and simple sources of up 10 100 MJ energy pulses and ultrastrong magnetic fields, has been found to be improved by "interception" of the magnetic flux while energy generated in one stage is transferred to and amplified in the next stage. As a general physical model of such generators is proposed a coaxial configuration of the outer primary solenoid and the inner secondary solenoid around the cylindrical liner containing a charge of condensed explosive substance. The initial magnetic flux inside the inner (secondary) solenoid is induced upon excitation of the outer (primary) solenoid by a current pulse from a discharging capacitor bank or another generator. As the current in this pulse reaches its maximum, an explosion is triggered inside the liner. The explosion products propel the liner, which then closes the secondary loop by "intercepting" the magnetic flux induced here by the primary solenoid. Electrical design and performance analysis of such a generator is based on a three-loop electrical model and Kirchhoff's circuit laws. A numerical solution of the circuit equations requires that the dynamic characteristics of all inductances be given. First is considered a generator with a lossless circuit and how the parameters of generated pulses on the secondary side depend on the capacitance of the excitation source on the primary side. Next is considered a generator with axial triggering of explosion, in which case the liner expands laterally and may be regarded as a single-turn solenoid with a changing radius. Finally are considered generators with a sliding contact. The results of theoretical evaluation are compared with experimental data, a cylindrical copper liner with a 70 mm diameter and a 1.5 mm wall thickness having been accelerated to a 2.2 km/s velocity inside a solenoid 104 mm in diameter. Figures 6; references 16.

Compaction of Ultrafine-Disperse TiN Under High Pressure

937J0109A Moscow DOKLADY AKADEMII NAUK in Russian Vol 331 No 3, Jul 93 (manuscript received 23 Mar 93) pp 306-307

[Article by R.A. Andreyevskiy, O.M. Grebtsova, Ye.P. Domashneva, I.A. Kiyanskiy, Ye.N. Kurkin, V.Ye. Perelman, V.I. Sinitsyn, O.D. Torbova, and V.I. Torbov, Institute of New Problems in Chemistry t Russian Academy of Sciences, Chernogolovka (Moscow Oblast), Russian Science Center "Kurchatov Institute," Moscow, Moscow Institute of Fine Chemical Technology imeni M.V. Lomonosov, and Experimental Design Office "Gorizont" (Horizon), Moscow; UDC 621.762]

[Abstract] An experimental study of ultrafine-disperse TiN powders was made concerning their compaction under high pressure. Two such powders were produced in a cold plasma by reaction of $TiCl_4$ and nitrogen, one in the presence of hydrogen (19.6 wt.% N, 0.37 wt.% C, 4 wt.% O) and one in the presence of TiH_2 (18.7 wt.% N, 0.24 wt.% C, 2.5 wt.% O). The first powder had a lattice period a= 0.4233 nm, an average grain diameter d $\approx$ 0.07 nm, a specific surface S= 16 m^2/g, a bulk density g= 0.27 g/cm^3 and a pycnometric density G= 5.18 g/cm^2. The second powder had a lattice period a= 0.430 nm, an average grain diameter d $\approx$ 0.08 nm, a specific surface S= 14 m^2 /g, a bulk density g= 0.37 g/cm^3 and a pycnometric density G= 0.37 g/cm^3. Each powder was poured into cylindrical and square molds, then compacted either by conventional static unilateral compression or in a high-pressure apparatus, under a pressure raised stepwise up to 7 GPa. They were also compacted by a pulsed magnetic field, with pulses of a few microseconds duration and 0.9 MG maximum strength equivalent to a pressure of about 3 GPa. The quite consistent and therefore reliable data indicate that the rate of compaction decreases appreciably as the pressure is raised above 1 GPa, pulsed compaction being less effective than static compaction under a pressure of 1 GPa but almost as effective under a pressure of 3 GPa. Noteworthy is a consistent difference in the compactibility of the two powders under any pressure within the given range, powder made in the presence of hydrogen becoming somewhat denser under the same pressure. This is attributable to its higher bulk density and to a stronger influence of intergranular friction on it. Modifying the mode of pressure application did not yield an appreciable improvement, but raising the temperature did: a porosity as low as 5% without significant grain growth was attained by compaction under a pressure within the 5-7 GPa range at 800°C. Figures 1; tables 1; reference 4.

Evolution of Homogeneous Isotropic Universe, Dark Mass, and Absence of Monopoles

937J0114A Moscow TEORETICHESKAYA I MATEMATICHESKAYA FIZIKA in Russian Vol 94 No 3, Mar 93 (manuscript received 10 Apr 92) pp 515-528

[Article by Yu.M. Loskutov, Moscow State University]

[Abstract] Some implications regarding the evolution of a homogeneous isotropic universe according to the field theory of gravitation (FTG) are refined for a better understanding of the nonrelativistic stage of its evolution and the "early" universe, it having already been shown that the scale factor R of such a universe varies periodically in time between a minimum and a maximum and that the dark mass is tens times larger than the the visible one. The energy-momentum tensor density of matter in the effective Riemann space is, as usually, approximated with the energy-momentum tensor density $T^{\alpha\gamma}$ of an "ideal" fluid. The square of the interval ds^2 in the effective Riemann space is expressed accordingly in terms of the Ricci tensor and the Minkowski metric, the still to be determined metric coefficients satisfying the fundamental system of FTG equations. To these equations are added the equations of matter dynamics. That system of FTG equations is then simplified by letting $g\epsilon = 1$ and $\lambda = 0$, and the expression for ds^2 transformed so as to include the coefficient $A^4R^2(\tau)$ in both the V-term and the Z-term. This model of a universe is physically realizable only if it also obeys the causality principle and thus satisfies the constraint $R(t) \leq A$ at every instant of time t. This constraint indicates that a boundlessly expanding Friedman universe is not a model realizable in the field theory of gravitation. The realizability of a model depends quite evidently on the value of constant A and the behavior of scale factor R. Further analysis of this stipulation and solution of equations indicate that field theory of gravitation admits only one and a pulsating model of universe evolution, if the graviton has a mass. When its mass is about 2.5×10^{-66} gram, then the density of matter fluctuates between about 10^{27} maximum and about minimum 1.25^{-30} g/cm^3 in endlessly repeating about 7.5×10^{10} year cycles in a permanently Euclidean space. The dark mass is then 25 times larger than the visible one and the highest temperature of matter in the state of maximum density is estimated at about 10^{12} GeV, thus several orders of magnitude lower than the Planck temperature of about 10^{19} GeV and too low for relict monopoles to be generated according to the Grand Unification Theory. If the graviton mass is zero, then the field theory of gravitation does not admit existence of a homogeneous isotropic universe. References 6.

Foreign Broadcast Information Service (FBIS) and Joint Publications Research Service (JPRS) publications contain political, military, economic, environmental, and sociological news, commentary, and other information, as well as scientific and technical data and reports. All information has been obtained from foreign radio and television broadcasts, news agency transmissions, newspapers, books, and periodicals. Items generally are processed from the first or best available sources. It should not be inferred that they have been disseminated only in the medium, in the language, or to the area indicated. Items from foreign language sources are translated; those from English-language sources are transcribed. Except for excluding certain diacritics, FBIS renders personal names and place-names in accordance with the romanization systems approved for U.S. Government publications by the U.S. Board of Geographic Names.

Headlines, editorial reports, and material enclosed in brackets [ ] are supplied by FBIS/JPRS. Processing indicators such as [Text] or [Excerpts] in the first line of each item indicate how the information was processed from the original. Unfamiliar names rendered phonetically are enclosed in parentheses. Words or names preceded by a question mark and enclosed in parentheses were not clear from the original source but have been supplied as appropriate to the context. Other unattributed parenthetical notes within the body of an item originate with the source. Times within items are as given by the source. Passages in boldface or italics are as published.

SUBSCRIPTION/PROCUREMENT INFORMATION

The FBIS DAILY REPORT contains current news and information and is published Monday through Friday in eight volumes: China, East Europe, Central Eurasia, East Asia, Near East & South Asia, Sub-Saharan Africa, Latin America, and West Europe. Supplements to the DAILY REPORTs may also be available periodically and will be distributed to regular DAILY REPORT subscribers. JPRS publications, which include approximately 50 regional, worldwide, and topical reports, generally contain less time-sensitive information and are published periodically.

Current DAILY REPORTs and JPRS publications are listed in *Government Reports Announcements* issued semimonthly by the National Technical Information Service (NTIS), 5285 Port Royal Road, Springfield, Virginia 22161 and the *Monthly Catalog of U.S. Government Publications* issued by the Superintendent of Documents, U.S. Government Printing Office, Washington, D.C. 20402.

The public may subscribe to either hardcover or microfiche versions of the DAILY REPORTs and JPRS publications through NTIS at the above address or by calling (703) 487-4630. Subscription rates will be provided by NTIS upon request. Subscriptions are available outside the United States from NTIS or appointed foreign dealers. New subscribers should expect a 30-day delay in receipt of the first issue.

U.S. Government offices may obtain subscriptions to the DAILY REPORTs or JPRS publications (hardcover or microfiche) at no charge through their sponsoring organizations. For additional information or assistance, call FBIS, (202) 338-6735,or write to P.O. Box 2604, Washington, D.C. 20013. Department of Defense consumers are required to submit requests through appropriate command validation channels to DIA, RTS-2C, Washington, D.C. 20301. (Telephone: (202) 373-3771, Autovon: 243-3771.)

Back issues or single copies of the DAILY REPORTs and JPRS publications are not available. Both the DAILY REPORTs and the JPRS publications are on file for public reference at the Library of Congress and at many Federal Depository Libraries. Reference copies may also be seen at many public and university libraries throughout the United States.

END OF FICHE

DATE FILMED

9 DEC 93